

Ground-state correlations of itinerant electrons in the spinless Falicov-Kimball chain and related tight-binding systems

Janusz Jędrzejewski^{1,2,*}, Taras Krokhmal'skii^{3,1,*} and Oleg Derzhko^{3,4,†}

¹Institute of Theoretical Physics, University of Wrocław

Max Born Sq. 9, 50-204 Wrocław, Poland

²Department of Theoretical Physics, University of Łódź

149/153 Pomorska Str., 90-236 Łódź, Poland

³Institute for Condensed Matter Physics

1 Svientsitskii Str., L'viv-11, 79011, Ukraine

⁴Chair of Theoretical Physics, Ivan Franko National University of L'viv

12 Drahomanov Str., L'viv-5, 79005, Ukraine

October 25, 2018

Abstract

We consider the one-dimensional spinless Falicov-Kimball model of itinerant fermionic particles (“spinless electrons”), which can hop between nearest-neighbour sites only, and of immobile particles (“classical ions”), with an on-site attraction. Extensive studies of the ground-state phase diagram of this system and its higher dimensional counterparts, carried out up to now, concentrated on determining ground-state arrangements of ions on the underlying lattice, while the properties of electrons were typically ignored. We report studies of short- and long-range correlations between electrons, and between ions and electrons, and of the spatial decay of electron correlations (decay of single-particle density matrix), in the ground state. The studies have been carried out analytically and by means of well-controlled numerical procedures. In the case of period 2 ground state, the single-particle density matrix has been expressed in terms of a hypergeometric function, and its spatial decay has been extracted. Numerical calculations have been done for open chains of various lengths (up to a few thousand sites), in order to control the chain-size dependence of correlations and to extrapolate the results to the limit of infinite chain. A part of the obtained results refers to tight-binding electrons subjected to a periodic external potential due to the ions, which constitute simple models of metals and insulators.

PACS numbers: 71.10.-w, 71.10.Fd

Keywords: spinless Falicov-Kimball chain, tight-binding electrons, ground state, short- and long-range correlation functions, single-particle density matrix, spatial decay of correlations

E-mail addresses:

★ — jjed@ift.uni.wroc.pl

* — krokhm@icmp.lviv.ua

† — derzhko@icmp.lviv.ua

1 Introduction

The Falicov-Kimball model emerged from solid-state theory in 1969, as a simple model for semiconductor-metal transitions [1]. Since that time it has become an important standard tool for studying various properties and phenomena that occur in strongly correlated fermionic systems, ranging from metal-insulator and mixed-valence phenomena to the Peierls instabilities and crystallization. For an overview and an extensive list of relevant references the reader is advised to consult [2, 3].

In the present paper we are studying the simplest, skeleton version of the model proposed by Falicov and Kimball, which is usually referred to as the spinless Falicov-Kimball model. This is a lattice system that consists of two sorts of spinless fermions, called electrons and ions. The electrons can hop between nearest-neighbour sites only, while the ions are immobile. The only interaction occurs between the electrons and ions and it is an on-site attraction of strength U . Throughout this paper, the underlying lattice is one-dimensional (later on called the chain), so it can be identified with integers \mathbb{Z} . When the chain is finite and consists of L sites labeled $x = 0, \dots, L - 1$, we impose *boundary conditions* b , which in this paper are either free ($b = f$) or periodic ($b = p$). Then, the whole two-component system is governed by the Hamiltonian:

$$H_b = - \sum_{x=0}^{L-1} (t_{b,x} a_x^+ a_{x+1} + t_{b,x} a_{x+1}^+ a_x + U w_x a_x^+ a_x), \quad (1)$$

where a_x^+ , a_x are the creation and annihilation operators of an electron at the site x of the chain, $t_{b,x}$ is the hopping rate between the sites x and $x + 1$ (which will be set site-independent, except at the boundary of a chain), and w_x stands for the occupation-number operator of an ion at site x . Since the occupation-number operators w_x commute with the Hamiltonian (1), we can identify them with classical variables taking values zero or one. Consequently the total number of ions, $N_i = \sum_x w_x$, is conserved. Moreover, the total particle-number operator of electrons, $\hat{N}_e = \sum_x a_x^+ a_x$, commutes with H_b , so the total number of electrons, N_e , is also conserved. Therefore, we can study the equilibrium properties of our system in the canonical ensemble, with a fixed number of sites L , the electron number N_e and the ion number N_i . The corresponding canonical partition function reads:

$$Z_b = \sum_{w: \sum_x w_x = N_i} \text{Tr}_{N_e} \exp(-\beta H_b), \quad (2)$$

where w stands for the function that to a site x of the underlying chain assigns the value $w_x = 0, 1$, which can be viewed as a sequence $w = w_0 w_1 \dots$ (hereafter called the *ion configuration*), the trace is over the Hilbert space of N_e electrons, and β is the inverse temperature.

Despite the apparent simplicity of the form of Hamiltonian (1) and its counterparts on higher-dimensional lattices \mathbb{Z}^d , $d > 1$, the question whether the system is capable of describing cooperative effects had remained open for almost two decades. It was affirmatively answered in 1986 [4, 5], by demonstrating that the half-filled system exhibits a staggered type of long-range order in the ionic subsystem at zero temperature, and showing that this staggered order persists at sufficiently low temperatures in two- and higher-dimensional systems [5].

Since then, one can observe an increased interest in the model and many properties of the Falicov-Kimball model have been established by means of rigorous methods as well as by means of various sorts of numerical procedures. Not surprisingly, a vast majority of obtained results refers to the ground state (see [2, 6, 3, 7] and references quoted there). As there are good reasons to believe that studies of the ground state of the one-dimensional model may reveal interesting cooperative phenomena, which herald the appearance of similar cooperative

phenomena in higher-dimensional systems at zero and sufficiently low temperatures, a lot of efforts at determining ground-state properties have been made [8]–[18].

As a matter of fact, all the attention, not only in the last quoted papers but also in many others whose references can be found in [2, 6, 3, 7], has been concentrated on the ionic subsystem. Specifically, the most favourable energetically ionic configurations and ionic correlations, at different values of the electron-ion coupling parameter U , have been determined. The problem of correlations between the itinerant fermionic particles had not been usually addressed. To the best of our knowledge, there are just a few exceptions. As mentioned in [2] the results on decay of superconducting correlations, obtained in [19, 20] for general itinerant-electron systems, can be applied to the ground state of the one-dimensional Falicov-Kimball model (1). In particular, it follows that the ground-state average of $a_x^\dagger a_y$ decays exponentially with the distance between the sites x and y , i.e. there is no so called off-diagonal long-range order. Similar results, but for multi-point products of fermionic creation and annihilation operators (that cannot be expressed in terms of occupation-number operators), have been obtained in the strong coupling regime in [21]. In [22] a class of models related with the spinless Falicov-Kimball model, with an emphasis on the static Holstein model, has been analyzed rigorously. As a byproduct of considerations carried out for the static Holstein model, the authors have obtained a relation between grand-canonical averages of one-site ion- and one-site electron-occupation numbers at half-filling. This result seems to be the first one referring to correlations between the electrons that can be expressed as an average of electron occupation-number operators. The mentioned relation implies that, at half-filling, the staggered long-range order in the ion subsystem is accompanied by the same kind of long-range order in the electron subsystem.

It should be emphasized here that we are concerned only with low-dimensional systems. There is an extensive literature concerning the limit of infinite dimensions, where calculations of some correlation functions, like linear-response functions, are quite common (see for instance [23]).

The purpose of this paper is to examine the properties of the electron subsystem of the model (1), at zero temperature. It is achieved by means of a number of short- and long-range correlation functions of electrons, and electrons and ions, that can be represented as canonical averages of operators constructed out of occupation-number operators of electrons and ions.

The paper is organized as follows. We start, in Section 2, with a brief discussion of canonical ground-state averages. In Section 3, we define and discuss some general properties of short- and long-range correlation functions, to be studied in the subsequent sections. Then, in Section 4, we present analytical results for closed finite chains and for infinite chains. After that, in Section 5, we give numerical results, obtained by means of numerical exact diagonalization. We end up, in Section 6, with a discussion and a summary of the obtained results.

2 The canonical ground state and ground-state averages

There are two approaches that enable one to study ground-state properties of a system. The first one is a quantum-mechanical approach, usually adopted in the papers concerning ground-state of Falicov-Kimball models, and consists in considering a finite (and then an infinite) system exclusively at zero temperature. The second one is a thermodynamic approach, where the considerations start with nonzero temperatures and then the limit of zero temperature is taken.

In the quantum-mechanical approach, one makes use of the fact, mentioned in Introduction, that a system of N_e electrons and N_i ions with Hamiltonian (1), confined to a chain (of L sites and with boundary conditions b), can be considered for a fixed ion configuration w . The

corresponding Hamiltonian, denoted $H_b(w)$, describes tight-binding electrons in the external potential $-Uw_x$. In this case, the ground state of N_e electrons, $|w\rangle_b$, that is the eigenvector of $H_b(w)$ to the lowest energy $E_b(w)$, is the so called *Fermi-sea state*. Then, the ground state of a finite chain with N_e electrons and N_i ions is given by the set G_b of *finite-chain ground-state ion configurations* g_b and the corresponding Fermi-sea states $|g_b\rangle_b$ of energy $E_b(g_b)$, such that

$$E_b(g_b) = \min_{w: \sum_x w_x = N_i} E_b(w). \quad (3)$$

To get thermodynamically relevant quantities, we first introduce the finite-chain ground-state energy densities:

$$e_b(w) = L^{-1}E_b(w), \quad e_b(g_b) = L^{-1}E_b(g_b) = \min_{w: \sum_x w_x = N_i} e_b(w), \quad (4)$$

for a given ion configuration w , and for given particle numbers N_e , N_i , respectively. Then, we go to the thermodynamic limit, denoted $\lim_{L \rightarrow \infty}$, i.e. we send L to infinity in such a way that the both ends of the chain (if any) become remote from any fixed site, and $L^{-1}N_e \rightarrow \rho_e$ – the electron density and $L^{-1}N_i \rightarrow \rho_i$ – the ion density, for some $\rho_e, \rho_i \in [0, 1]$. In the thermodynamic limit and for a fixed ion (infinite-chain) configuration w , the (infinite-chain) ground-state energy density is

$$e(w) = \lim_{L \rightarrow \infty} e_b(w), \quad (5)$$

and is independent of boundary conditions. In the r.h.s of (5), the ion configuration w stands for the restriction of the infinite-chain configuration w to the finite chain. For given particle densities ρ_e, ρ_i , the *infinite-chain ground-state energy density*, e , is

$$e = \min_w e(w) = e(g), \quad g \in G, \quad (6)$$

where the minimum is taken over infinite-chain configurations of ions and the set G , defined by (6), stands for the set of *infinite-chain ground-state ion configurations*. Alternatively, the ground-state energy density can be obtained as

$$e = \lim_{L \rightarrow \infty} e_b(g_b), \quad g_b \in G_b. \quad (7)$$

In the thermodynamic approach, we start with nonzero temperatures and define the finite-chain internal-energy density $e_{\beta,b}$,

$$e_{\beta,b} = L^{-1} \langle H_b \rangle_{\beta,b}, \quad (8)$$

where

$$\langle H_b \rangle_{\beta,b} = Z_b^{-1} \sum_{w: \sum_x w_x = N_i} \text{Tr}_{N_e} H_b \exp(-\beta H_b) \quad (9)$$

is the canonical average of H_b . Then, the (infinite-chain) internal-energy density, e_β , is given by $e_\beta = \lim_{L \rightarrow \infty} e_{\beta,b}$, and is independent of boundary conditions. Thermodynamically, the ground-state energy density, e , equals to $e = \lim_{\beta \rightarrow \infty} e_\beta$. Reversing the order of the limits $L \rightarrow \infty, \beta \rightarrow \infty$, we recover the formula (7) of the quantum-mechanical approach

$$e = \lim_{L \rightarrow \infty} e_b(g_b), \quad e_b(g_b) = \lim_{\beta \rightarrow \infty} e_{\beta,b} = L^{-1} {}_b \langle g_b | H_b | g_b \rangle_b, \quad g_b \in G_b. \quad (10)$$

To define a ground-state average, we start with nonzero temperatures. Let A be an operator built out of a_x^+ , a_x and/or w_x , depending on a finite number of sites only. By definition, the finite-chain canonical average of A , $\langle A \rangle_{\beta,b}$, is

$$\langle A \rangle_{\beta,b} = Z_b^{-1} \sum_{w: \sum_x w_x = N_i} \text{Tr}_{N_e} A \exp(-\beta H_b). \quad (11)$$

The infinite-chain limit of $\langle A \rangle_{\beta,b}$ amounts to the canonical average of A , $\langle A \rangle_{\beta}$,

$$\lim_{L \rightarrow \infty} \langle A \rangle_{\beta,b} = \langle A \rangle_{\beta}, \quad (12)$$

which is independent of boundary conditions and translation invariant. Then, the *infinite-chain ground-state average* of A , $\langle A \rangle$, is defined as

$$\lim_{\beta \rightarrow \infty} \langle A \rangle_{\beta} = \langle A \rangle. \quad (13)$$

The ground-state average $\langle A \rangle$ shares the above mentioned properties of $\langle A \rangle_{\beta}$.

By rigorous results of [14] and numerical results of [12, 13, 17], for pairs of rational densities (ρ_e, ρ_i) , satisfying a linear relation, and for suitable values of electron-ion attraction U , the set G of ground-state configurations of ions consists of a finite number of elements. This happens, for instance, if $\rho_e = p/q$, where the natural numbers p and q are relatively prime, and $\rho_i = \rho_e$ (the so called neutral case), for sufficiently large U [12, 13]. Then, G consists of q periodic configurations of period q (the so called most homogeneous configurations) that differ from each other by a translation. In such a case, the ground-state average of A equals to

$$\langle A \rangle = q^{-1} \sum_{g \in G} \lim_{L \rightarrow \infty} {}_b \langle g|A|g \rangle_b, \quad (14)$$

where g in $|g\rangle_b$ stands for the restriction of a $g \in G$ to the finite chain. As a finite-chain approximation to $\langle A \rangle$, converging to $\langle A \rangle$ as $L \rightarrow \infty$, we choose $\langle A \rangle_b$ given by

$$\langle A \rangle_b = q^{-1} \sum_{g \in G} {}_b \langle g|A|g \rangle_b. \quad (15)$$

In what follows, we refer to the ground-state average (15) as the *symmetric average*, while the quantum average ${}_b \langle g|A|g \rangle_b$ is called the *broken-symmetry average*. Since the quantum averages ${}_b \langle g|A|g \rangle_b$ appear frequently throughout the paper, we introduce the abbreviated notation $\langle A \rangle_{b,g} \equiv {}_b \langle g|A|g \rangle_b$. In general, a finite set of Q ground-state configurations G may consist of configurations related by translations and reflections, with $Q \geq q$.

3 Short- and long-range correlation functions: definitions, general properties, and the method of calculation

Throughout the sections that follow, the set G stands for the set of periodic ground-state configurations of the infinite chain, for given $\rho_e = p/q$, with p and q being relatively prime natural numbers, $\rho_i = m\rho_e$, with $m = 1, 2, \dots$, and for suitable values of U . Later on, the set of U for which G is the set of the ground-state configurations will be called the *stability interval* of G , and denoted ΔU_G . The set G consists of q ion configurations, with period q , which are known as the atomic ($m = 1$) or m -*molecular* ($m \geq 2$) *most homogeneous ion configurations* [14, 12, 13]. Following [13], the set of m -molecule most homogeneous configurations corresponding to the electron density $\rho_e = p/q$ is denoted $[p/q]_m$. The elements of $[p/q]_m$ can conveniently be described by specifying their restriction to the unit cell, whose sites are labeled $x = 0, 1, \dots, q-1$, i.e. as a sequence $g = g_0 g_1 \dots g_{q-1}$. The positions of ions in the unit cell of the *representative configuration* of $[p/q]_m$ can be obtained as the solutions k_j to the equations:

$$pk_j = j \pmod{q}, \quad j = 0, 1, \dots, mp - 1. \quad (16)$$

The remaining $q - 1$ configurations of $[p/q]_m$ are obtained by translating the defined above representative configuration.

Moreover, the number of sites in the chain, L , is set to be a multiple of q , so that $L^{-1}N_e = \rho_e$, and $L^{-1}N_i = \rho_i$. For the ion subsystem the correlation functions are defined in Appendix A. Below, we define analogous correlation functions for the electron subsystem. The list of correlation functions, studied in the sections that follow, opens a one-point function, the *local electron density in the ion configuration* g :

$$\langle n_x \rangle_{b,g}, \quad g \in G. \quad (17)$$

It is related to ρ_e by

$$L^{-1} \sum_x \langle n_x \rangle_{b,g} = \rho_e. \quad (18)$$

For periodic boundary conditions ($b = p$), $\langle n_x \rangle_{p,g}$ has period q : $\langle n_x \rangle_{p,g} = \langle n_{x+q} \rangle_{p,g}$, and

$$\rho_e = \langle n_x \rangle_p = q^{-1} \sum_{g \in G} \langle n_x \rangle_{p,g} = q^{-1} \sum_{y=0}^{q-1} \langle n_{x+y} \rangle_{p,g}. \quad (19)$$

Then, we consider a number of two-point correlation functions. The first one is the *density-density correlation in the ion configuration* g , $\langle n_x n_y \rangle_{b,g}$, which (by the Wick's theorem) can be expressed as

$$\langle n_x n_y \rangle_{b,g} = \langle n_x \rangle_{b,g} \langle n_y \rangle_{b,g} - |\langle a_x^+ a_y \rangle_{b,g}|^2. \quad (20)$$

For the periodic boundary conditions, $\langle n_x n_y \rangle_{p,g}$ has period q , $\langle n_x n_y \rangle_p$ is translation invariant, and the symmetric average $\langle (n_x - \rho_e)(n_y - \rho_e) \rangle_p$ can be written as follows

$$\begin{aligned} \langle (n_x - \rho_e)(n_y - \rho_e) \rangle_p &= q^{-1} \sum_{g \in G} \langle n_x n_y \rangle_{p,g} - \rho_e^2 \\ &= q^{-1} \sum_{g \in G} \langle n_x - \rho_e \rangle_{p,g} \langle n_y - \rho_e \rangle_{p,g} - q^{-1} \sum_g |\langle a_x^+ a_y \rangle_{p,g}|^2. \end{aligned} \quad (21)$$

The symmetric average of the above kind is used to define the *electron-electron short-range correlation function*, $\mathcal{L}_{b,x}(l)$,

$$\mathcal{L}_{b,x}(l) = \langle (n_x - \rho_e)(n_{x+l} - \rho_e) \rangle_b. \quad (22)$$

In an analogous manner, we define the *electron-ion short-range correlation function*, $\mathcal{S}_{b,x}(l)$:

$$\mathcal{S}_{b,x}(l) = q^{-1} \sum_{g \in G} \langle (g_x - mn_x)(g_{x+l} - mn_{x+l}) \rangle_{b,g}. \quad (23)$$

In the case of the periodic boundary conditions, the correlation functions, $\mathcal{L}_{b,x}(l)$ and $\mathcal{S}_{b,x}(l)$, are translation invariant (i.e. depend only on l). To define the long-range correlations corresponding to the above short-range correlations, we start with the *order-parameter operators* \hat{O}_k , \hat{O}_g , and $\hat{O}_{g,g'}$:

$$\hat{O}_k = L^{-1} \sum_{x=0}^{L-1} e^{ikx} (n_x - \rho_e), \quad (24)$$

$$\hat{O}_g = L^{-1} \sum_{x=0}^{L-1} (g_x - \rho_i) (n_x - \rho_e), \quad (25)$$

and

$$\hat{O}_{g,g'} = L^{-1} \sum_{x=0}^{L-1} (g_x - \rho_i) (g'_x - mn_x). \quad (26)$$

Taking broken-symmetry averages of the order-parameter operators, we obtain the corresponding *order parameters*:

$$\langle \hat{O}_k \rangle_{b,g} = L^{-1} \sum_{x=0}^{L-1} e^{ikx} \langle n_x - \rho_e \rangle_{b,g}, \quad (27)$$

$$\langle \hat{O}_g \rangle_{b,g'} = L^{-1} \sum_{x=0}^{L-1} (g_x - \rho_i) \langle n_x - \rho_e \rangle_{b,g'}. \quad (28)$$

and

$$\langle \hat{O}_{g,g'} \rangle_{b,g'} = L^{-1} \sum_{x=0}^{L-1} (g_x - \rho_i) \langle g'_x - mn_x \rangle_{b,g'}. \quad (29)$$

The symmetric averages of the order-parameter operators vanish:

$$\langle \hat{O}_k \rangle_b = \langle \hat{O}_g \rangle_b = q^{-1} \sum_{g' \in G} \langle \hat{O}_{g,g'} \rangle_{b,g'} \equiv 0. \quad (30)$$

By means of the order-parameter operators we define the *long-range correlation functions* $\mathcal{P}_b(k)$, \mathcal{L}_b , and \mathcal{S}_b :

$$\begin{aligned} \mathcal{P}_b(k) &\equiv \langle \hat{O}_k^+ \hat{O}_k \rangle_b \\ &= L^{-2} \sum_{x,y=0}^{L-1} e^{ik(x-y)} \langle (n_x - \rho_e) (n_y - \rho_e) \rangle_b, \end{aligned} \quad (31)$$

$$\begin{aligned} \mathcal{L}_b &\equiv q^{-1} \sum_{g \in G} \langle \hat{O}_g^2 \rangle_b \\ &= L^{-2} \sum_{x,y=0}^{L-1} q^{-1} \sum_{g \in G} [(g_x - \rho_i) (g_y - \rho_i)] \langle (n_x - \rho_e) (n_y - \rho_e) \rangle_b, \end{aligned} \quad (32)$$

and

$$\begin{aligned} \mathcal{S}_b &\equiv q^{-2} \sum_{g,g' \in G} \langle \hat{O}_{g,g'}^2 \rangle_{b,g'} \\ &= L^{-2} \sum_{x,y=0}^{L-1} q^{-1} \sum_{g \in G} [(g_x - \rho_i) (g_y - \rho_i)] q^{-1} \sum_{g' \in G} \langle (g'_x - mn_x) (g'_y - mn_y) \rangle_{b,g'}. \end{aligned} \quad (33)$$

In the case of the periodic boundary conditions, the long-range correlation functions $\mathcal{P}_p(k)$, \mathcal{L}_p , and \mathcal{S}_p assume the form

$$\mathcal{P}_p(k) = L^{-1} \sum_{l=0}^{L-1} e^{-ikl} \mathcal{L}_p(l), \quad (34)$$

$$\mathcal{L}_p = L^{-1} \sum_{l=0}^{L-1} E_p(l) \mathcal{L}_p(l), \quad (35)$$

$$\mathcal{S}_p = L^{-1} \sum_{l=0}^{L-1} E_p(l) \mathcal{S}_p(l), \quad (36)$$

where $\mathcal{L}_p(l) \equiv \mathcal{L}_{p,x}(l)$, $\mathcal{S}_p(l) \equiv \mathcal{S}_{p,x}(l)$, and $E_p(l)$ is defined in Appendix A. The function $k \rightarrow \mathcal{P}_p(k)$ is usually referred to as the *static structure factor* [25]. Since, the following relations hold,

$$\begin{aligned} \langle \hat{O}_k^+ \hat{O}_k \rangle_{b,g} &= L^{-2} \sum_{x,y=0}^{L-1} e^{ik(x-y)} \langle n_x - \rho_e \rangle_{b,g} \langle n_y - \rho_e \rangle_{b,g} \\ &\quad - L^{-2} \sum_{x,y=0}^{L-1} e^{ik(x-y)} |\langle a_x^+ a_y \rangle_{b,g}|^2, \end{aligned} \quad (37)$$

$$\begin{aligned} \langle \hat{O}_g^2 \rangle_{b,g'} &= L^{-2} \sum_{x,y=0}^{L-1} (g_x - \rho_i) (g_y - \rho_i) \langle n_x - \rho_e \rangle_{b,g'} \langle n_y - \rho_e \rangle_{b,g'} \\ &\quad - L^{-2} \sum_{x,y=0}^{L-1} (g_x - \rho_i) (g_y - \rho_i) |\langle a_x^+ a_y \rangle_{b,g'}|^2, \end{aligned} \quad (38)$$

and

$$\begin{aligned} \langle \hat{O}_{g,g'}^2 \rangle_{b,g'} &= L^{-2} \sum_{x,y=0}^{L-1} (g_x - \rho_i) (g_y - \rho_i) \langle g'_x - mn_x \rangle_{b,g'} \langle g'_y - mn_y \rangle_{b,g'} \\ &\quad - L^{-2} \sum_{x,y=0}^{L-1} (g_x - \rho_i) (g_y - \rho_i) |\langle a_x^+ a_y \rangle_{b,g'}|^2, \end{aligned} \quad (39)$$

and since, for periodic boundary conditions, the averages $\langle \hat{O}_g^2 \rangle_p$, $q^{-1} \sum_{g' \in G} \langle \hat{O}_{g,g'}^2 \rangle_{p,g'}$, and $\langle \hat{O}_k^+ \hat{O}_k \rangle_{p,g}$ are translation invariant, hence independent of $g \in G$,

$$\mathcal{P}_p(k) \equiv \langle \hat{O}_k^+ \hat{O}_k \rangle_p = |\langle \hat{O}_k \rangle_{p,g}|^2 - L^{-1} \sum_{l=0}^{L-1} e^{-ikl} |\langle a_x^+ a_{x+l} \rangle_{p,g}|^2, \quad (40)$$

$$\begin{aligned} \mathcal{L}_p &\equiv q^{-1} \sum_{g \in G} \langle \hat{O}_g^2 \rangle_p = q^{-1} \sum_{g' \in G} \left(\langle \hat{O}_g \rangle_{p,g'} \right)^2 \\ &\quad - L^{-1} \sum_{l=0}^{L-1} (g_x - \rho_i) (g_{x+l} - \rho_i) q^{-1} \sum_{g' \in G} |\langle a_x^+ a_{x+l} \rangle_{p,g'}|^2, \end{aligned} \quad (41)$$

and

$$\begin{aligned} \mathcal{S}_p \equiv q^{-2} \sum_{g,g' \in G} \langle \hat{O}_{g,g'}^2 \rangle_{p,g'} &= q^{-1} \sum_{g' \in G} \langle \hat{O}_{g,g'}^2 \rangle_{p,g'} = q^{-1} \sum_{g' \in G} \left(\langle \hat{O}_{g,g'} \rangle_{p,g'} \right)^2 \\ &\quad - L^{-1} \sum_{l=0}^{L-1} (g_x - \rho_i) (g_{x+l} - \rho_i) q^{-1} \sum_{g' \in G} |\langle a_x^+ a_{x+l} \rangle_{p,g'}|^2. \end{aligned} \quad (42)$$

For the one-dimensional systems of the kind considered here, and in the limit $L \rightarrow \infty$, the second term in (40), (41), (42) vanishes (see [19, 20] and the sections that follow). Thus, in the thermodynamic limit we find simple relations between long-range correlations and the corresponding order parameters

$$\mathcal{P}(k) \equiv \lim_{L \rightarrow \infty} \mathcal{P}_p(k) = \lim_{L \rightarrow \infty} \langle \hat{O}_k^+ \hat{O}_k \rangle_p = \left| \lim_{L \rightarrow \infty} \langle \hat{O}_k \rangle_{p,g} \right|^2, \quad (43)$$

$$\mathcal{L} \equiv \lim_{L \rightarrow \infty} \mathcal{L}_p = q^{-1} \sum_{g' \in G} \left(\lim_{L \rightarrow \infty} \langle \hat{O}_g \rangle_{p,g'} \right)^2, \quad (44)$$

and

$$\mathcal{S} \equiv \lim_{L \rightarrow \infty} \mathcal{S}_p = q^{-1} \sum_{g' \in G} \left(\lim_{L \rightarrow \infty} \langle \hat{O}_{g,g'} \rangle_{p,g'} \right)^2. \quad (45)$$

The relations (43), (44), (45) hold for other boundary conditions as well. If the quantities $\mathcal{P}(k)$, \mathcal{L} are strictly positive, one says that the considered system exhibits the *long-range order*.

In order to calculate the correlation functions defined above, one can use the fact that for a fixed ion configuration w the Hamiltonian of the system, $H_b(w)$, is a second quantized form of the one-electron Hamiltonian $h_b(w)$. If we denote by $\{|x\rangle\}_{x=0,\dots,L-1}$ the orthogonal basis of one-electron states, such that a_x^+ creates an electron in the state $|x\rangle$, then the matrix elements of $h_b(w)$ in the basis $\{|x\rangle\}_{x=0,\dots,L-1}$ are defined by

$$H_b(w) = \sum_{x,y=0}^{L-1} \langle x|h_b(w)|y\rangle a_x^+ a_y, \quad (46)$$

i.e. explicitly, all the non-vanishing matrix elements are given by

$$\langle x|h_b(w)|x\rangle = -Uw_x, \quad \langle x|h_b(w)|y\rangle = -t_{b,x} \quad \text{if } y = x \pm 1. \quad (47)$$

Let $\{|v\rangle\}_{v=v_0,\dots,v_{L-1}}$ be the orthonormal basis built out of the eigenstates of $h_b(w)$ to the eigenvalues Λ_v , such that $\Lambda_v \leq \Lambda_{v'}$ if $v < v'$. Then, the unitary matrix \mathcal{U} , with the following matrix elements \mathcal{U}_{xv} :

$$\mathcal{U}_{xv} = \langle x|v\rangle, \quad (48)$$

diagonalizes the matrix of $h_b(w)$,

$$\sum_{x,y} \mathcal{U}_{vy}^+ \langle y|h_b(w)|x\rangle \mathcal{U}_{xv'} = \Lambda_v \delta_{vv'}. \quad (49)$$

Moreover, the set of operators $\{b_v^+, b_v\}$, $v = v_0, \dots, v_{L-1}$, defined by

$$b_v = \sum_{x=0}^{L-1} \langle v|x\rangle a_x, \quad (50)$$

satisfies the canonical anticommutation relations, and

$$H_b(w) = \sum_{x,y=0}^{L-1} \langle x|h_b(w)|y\rangle a_x^+ a_y = \sum_v \Lambda_v b_v^+ b_v. \quad (51)$$

Since,

$$a_x = \sum_v \langle x|v\rangle b_v, \quad (52)$$

we can express the basic electron-correlation functions, $\langle n_x \rangle$, $\langle a_x^+ a_y \rangle_{b,w}$, and $\langle n_x n_y \rangle_{b,w}$, in terms of the site-components $\langle x|v\rangle$ of the eigenvectors $|v\rangle$:

$$\begin{aligned} \langle n_x \rangle_{b,w} &\equiv {}_b \langle w|a_x^+ a_x|w\rangle_b = \sum_{v \leq v_F} |\langle x|v\rangle|^2, \\ \langle a_x^+ a_y \rangle_{b,w} &\equiv {}_b \langle w|a_x^+ a_y|w\rangle_b = \sum_{v \leq v_F} \langle v|x\rangle \langle y|v\rangle, \\ \langle n_x n_y \rangle_{b,w} &\equiv {}_b \langle w|a_x^+ a_x a_y^+ a_y|w\rangle_b = \sum_{v \leq v_F} |\langle x|v\rangle|^2 \sum_{v \leq v_F} |\langle y|v\rangle|^2 \\ &\quad - \left| \sum_{v \leq v_F} \langle v|x\rangle \langle y|v\rangle \right|^2, \end{aligned} \quad (53)$$

where v_F stands for the label of eigenvectors $|v\rangle$, such that there is exactly N_e eigenvectors with $v \leq v_F$. Consequently, all the correlation functions defined in this section can be expressed in terms of the site-components $\langle x|v\rangle$ of the eigenvectors of $h_b(w)$. For some low-period ion configurations the eigenproblem can be solved exactly, while for any other ground-state configurations of interest, and arbitrary boundary conditions, one can resort to numerical exact-diagonalization procedures.

4 Correlation functions – exact results

In this section, we calculate exactly ground-state correlation functions of a finite chain with the periodic boundary conditions only (so without any risk of confusion the subscript p by the averages can be dropped), and then the infinite-chain limits, in two cases.

First, for completeness, when $\rho_e \in [0, 1]$ and $\rho_i = 0$. For such a particle densities, G consist of a single ion configuration, called the *empty configuration*, for any U . In this configuration, $g_x = 0$ for all x , so we denote it $g \equiv 0$.

Second, when $\rho_e = 1/2$ and $\rho_i = 1/2$, and $G = [1/2]_1$ consists of the two *checkerboard configurations*: $\text{ch}^1 = 10$ and $\text{ch}^2 = 01$. This holds also for any nonzero U , i.e. $\Delta U_{[1/2]_1} = (0, \infty)$ [5].

When $g_x = 0$ for all x , all the non-vanishing matrix elements of $h_p(0)$ are given by

$$\langle x|h_p(0)|x+1\rangle = -t_{p,x}, \quad t_{p,x} = 1, \quad x = 0, 1, \dots, L-1, \quad (54)$$

Let $k \in \{2\pi l/L : l = 0, 1, \dots, L-1\}$, so that for any L , $0 \leq k < 2\pi$. The eigenvectors of $h_p(0)$, denoted $|k\rangle$, are specified by their site components, $\langle x|k\rangle$,

$$\langle x|k\rangle = L^{-1/2} e^{ikx}, \quad (55)$$

while the corresponding eigenvalues, ε_k , read

$$\varepsilon_k = -2 \cos k. \quad (56)$$

Introducing $k_F = \pi(N_e - 1)/L$, we obtain

$$\langle a_x^\dagger a_{x+l} \rangle_0 = \frac{1}{L} \sum_{\substack{k \leq k_F, \\ k \geq 2\pi - k_F}} \exp(ikl) = \frac{1}{L} \left[1 + 2 \sum_{0 < k \leq k_F} \cos(kl) \right] = \frac{1}{L} \frac{\sin(\pi l N_e / L)}{\sin(\pi l / L)}. \quad (57)$$

Thus, in the infinite-chain limit

$$\lim_{L \rightarrow \infty} |\langle a_x^\dagger a_{x+l} \rangle_0|^2 = \frac{1}{\pi^2} \frac{\sin^2(\pi \rho_e l)}{l^2}, \quad (58)$$

$$\lim_{L \rightarrow \infty} \langle n_x n_{x+l} \rangle_0 = \rho_e^2 - \frac{1}{\pi^2} \frac{\sin^2(\pi \rho_e l)}{l^2}. \quad (59)$$

The analogous expressions for continuous counterparts of our system can be found in [24, 25]. The case of open boundary conditions has been considered in detail in [26]. Let us mention that the expression for the density-density correlation function $\langle n_x n_{x+l} \rangle$, obtained in [26], differs from our result (59), since the limit $L \rightarrow \infty$ is constructed in a different way, namely as the limit of half-infinite chain (only one end becomes remote from a fixed site).

More interesting is, of course, the case of the checkerboard ground-state configurations $g = \text{ch}^1, \text{ch}^2$, which are related by the primitive translation of the chain. In this case, all the non-vanishing matrix elements of $h_p(\text{ch}^1)$ are given by

$$\langle x | h_p(\text{ch}^1) | x+1 \rangle = -t_{p,x} = -1, \quad \langle x | h_p(\text{ch}^1) | x \rangle = -U \text{ch}_x^1. \quad (60)$$

In the basis $\{|k_0\rangle, |k_0 + \pi\rangle, |k_1\rangle, |k_1 + \pi\rangle, \dots\}$, $k = 2\pi l/L$, $l = 0, 1, \dots, L/2 - 1$, obtained by reordering the basis $\{|k\rangle\}$, the matrix of $h_p(\text{ch}^1)$ becomes block-diagonal. The diagonal blocks are 2 by 2 matrices $[h_p(\text{ch}^1)]_k$ that in the basis $\{|k\rangle, |k + \pi\rangle\}$ assume the form

$$[h_p(\text{ch}^1)]_k = \begin{bmatrix} \varepsilon_k - \frac{U}{2} & -\frac{U}{2} \\ -\frac{U}{2} & -\varepsilon_k - \frac{U}{2} \end{bmatrix}.$$

Thus, we obtain easily the eigenvalues, $\Lambda_\pm(k)$,

$$\Lambda^\pm(k) = -\frac{U}{2} \pm \Delta, \quad \Delta = \sqrt{\varepsilon_k^2 + \alpha^2}, \quad \alpha = \frac{U}{2}, \quad (61)$$

and the corresponding eigenvectors, $|k\rangle_{ch}^\pm$, given by:

$$[h_p(\text{ch}^1)]_k |k\rangle_{ch}^\pm = \Lambda^\pm(k) |k\rangle_{ch}^\pm, \quad (62)$$

and

$$|k\rangle_{ch}^\pm = (\gamma_k^\pm)^{-1} (\alpha |k\rangle + \beta_k^\pm |k + \pi\rangle), \quad \beta_k^\pm = \varepsilon_k \mp \Delta, \quad (63)$$

where the normalizing factor γ_k^\pm is

$$(\gamma_k^\pm)^2 \equiv \alpha^2 + (\beta_k^\pm)^2 = 2\Delta\beta_k^\pm. \quad (64)$$

Since in what follows, we shall be interested in $\rho_e \leq 1/2$ only, we can restrict our considerations to the lowest $L/2$ eigenvalues $\Lambda^-(k)$ and the corresponding eigenvectors $|k\rangle^-$, and set

$$|k\rangle_{ch} \equiv |k\rangle_{ch}^-, \quad \beta_k \equiv \beta_k^- = \varepsilon_k + \Delta, \quad \gamma_k \equiv \gamma_k^-. \quad (65)$$

Then, the site-components of eigenvectors $|k\rangle_{ch}$ read

$$\langle x|k\rangle_{ch} = \frac{1}{\sqrt{L}} \frac{1}{\gamma_k} (\alpha e^{ikx} + \beta_k e^{i(k+\pi)x}), \quad (66)$$

and consequently, setting $\langle \text{ch}^1 | a_x^+ a_x | \text{ch}^1 \rangle \equiv \langle a_x^+ a_x \rangle_1$, the local density $\langle n_x \rangle_1$ reads

$$\langle n_x \rangle_1 = \langle a_x^+ a_x \rangle_1 = \frac{1}{L} \sum_{\substack{k \leq k_F, \\ k \geq \pi - k_F}} |\langle x|k\rangle_{ch}|^2 = \rho_e + (-1)^x \alpha \tau_0(0), \quad (67)$$

where

$$\tau_0(l) \equiv \frac{1}{L} \left\{ \frac{1}{\sqrt{4 + \alpha^2}} + 2 \sum_{0 < k \leq k_F} \frac{\cos(kl)}{\Delta} \right\}. \quad (68)$$

In the thermodynamic limit,

$$\begin{aligned} \lim_{L \rightarrow \infty} \tau_0(l) &= \frac{1}{\pi} \int_0^{\pi \rho_e} dk \frac{\cos(kl)}{\Delta} \\ &= \frac{1}{\pi} \int_0^{\pi \rho_e} dk \frac{\cos(kl)}{\sqrt{\alpha^2 + \varepsilon_k^2}} = \frac{\kappa}{2\pi} \int_0^{\pi \rho_e} dk \frac{\cos(kl)}{\sqrt{1 - \kappa^2 \sin^2 k}}, \quad \rho_e \leq \frac{1}{2}, \quad \kappa^2 = \frac{1}{1 + (\frac{U}{4})^2} < 1. \end{aligned} \quad (69)$$

Since, the function $\lim_{L \rightarrow \infty} \tau_0(l)$ appears in many expressions for correlation functions, in the sequel, it is interesting to see its dependence on ρ_e and U . This is shown in Fig. 1. The analytic expressions for the asymptotic behaviour of this function, for $U \rightarrow 0$ and for $U \rightarrow \infty$, are given in Appendix B. Using these asymptotic formulae we find the corresponding asymptotic expressions for the local density $\langle n_x \rangle_1$: for $U \rightarrow 0$

$$\lim_{L \rightarrow \infty} \langle n_x \rangle_1 \approx \begin{cases} \rho_e + (-1)^x \alpha (2\pi)^{-1} \ln \tan [\pi(1 + 2\rho_e)/4], & \rho_e < \frac{1}{2}, \\ \rho_e + (-1)^x \alpha (2\pi)^{-1} (a_0 + 2 \ln 2 - \ln \alpha), & \rho_e = \frac{1}{2}, \end{cases} \quad (70)$$

while for $U \rightarrow \infty$ and any $\rho_e \leq 1/2$,

$$\lim_{U \rightarrow \infty} \lim_{L \rightarrow \infty} \langle n_x \rangle_1 = \rho_e + (-1)^x \rho_e, \quad (71)$$

which in the case of half-filling (i.e. for $\rho_e = 1/2$) amounts to ch^1 . Moreover, in the case of half-filling, the local electron-density of an infinite chain can be expressed by the complete elliptic integral of the first kind K [27], at the point κ^2 ,

$$\langle n_x \rangle_1 = \frac{1}{2} + (-1)^x \frac{U\kappa}{4\pi} \int_0^{\pi/2} \frac{dk}{\sqrt{1 - \kappa^2 \sin^2 k}} = \frac{1}{2} + (-1)^x \frac{U\kappa}{4\pi} K(\kappa^2), \quad \rho_e = \frac{1}{2}. \quad (72)$$

Now, consider the two-point correlation function $\langle a_x^+ a_{x+l} \rangle_1 \equiv \langle \text{ch}^1 | a_x^+ a_{x+l} | \text{ch}^1 \rangle_{\text{ch}}$. For $\rho_e \leq 1/2$, we find

$$\begin{aligned} \langle a_x^+ a_{x+l} \rangle_1 &= \sum_{\substack{k \leq k_F, \\ k \geq \pi - k_F}} {}_1 \langle k|x \rangle \langle x+l|k \rangle_1 \\ &= \frac{1}{L} \sum_{\substack{k \leq k_F, \\ k \geq \pi - k_F}} \frac{e^{ikl}}{\gamma_k^2} \{ \alpha^2 + (-1)^l \beta_k^2 + (-1)^x \alpha \beta_k [1 + (-1)^l] \}, \end{aligned} \quad (73)$$

which for nonzero and even l assumes the form

$$\begin{aligned} l = 2s, \quad s = 1, 2, \dots, \quad \langle a_x^+ a_{x+l} \rangle_1 &= \frac{1}{L} \sum_{\substack{k \leq k_F, \\ k \geq \pi - k_F}} e^{ikl} \left(1 + (-1)^x \frac{\alpha}{\Delta} \right) \\ &= \langle a_x^+ a_{x+l} \rangle_0 + (-1)^x \alpha \frac{1}{L} \left\{ \frac{1}{\sqrt{4 + \alpha^2}} + 2 \sum_{0 < k \leq k_F} \frac{\cos(kl)}{\Delta} \right\} \equiv \langle a_x^+ a_{x+l} \rangle_0 + (-1)^x \alpha \tau_0(2s), \end{aligned} \quad (74)$$

while for odd l , the form:

$$\langle a_x^+ a_{x+l} \rangle_1 = \frac{1}{L} \sum_{\substack{k \leq k_F, \\ k \geq \pi - k_F}} e^{ikl} \left(-\frac{\varepsilon_k}{\Delta} \right) = \tau_1(l), \quad l = 2s + 1, \quad s = 0, 1, \dots, \quad (75)$$

where

$$\tau_1(l) \equiv \frac{1}{L} \left\{ \frac{2}{\sqrt{4 + \alpha^2}} + 2 \sum_{0 < k \leq k_F} \cos(kl) \left(-\frac{\varepsilon_k}{\Delta} \right) \right\}. \quad (76)$$

We note that the functions τ_0 and τ_1 satisfy the relation:

$$\tau_1(2s + 1) = \tau_0(2s + 2) + \tau_0(2s). \quad (77)$$

Summarizing, for $\rho_e \leq 1/2$, the two-point function $\langle a_x^+ a_{x+l} \rangle_1$ reads

$$\langle a_x^+ a_{x+l} \rangle_1 = \begin{cases} \tau_1(l), & l = 2s + 1, \quad s = 0, 1, \dots, \\ \langle a_x^+ a_{x+l} \rangle_0 + (-1)^x \alpha \tau_0(l), & l = 2s, \quad s = 1, 2, \dots \end{cases} \quad (78)$$

As expected, since for $U \rightarrow 0$: $\tau_1(l) \rightarrow \langle a_x^+ a_{x+l} \rangle_0$, and $\alpha \lim_{L \rightarrow \infty} \tau_0(l) \rightarrow 0$ (see Appendix B), the two-point function $\langle a_x^+ a_{x+l} \rangle_1 \rightarrow \langle a_x^+ a_{x+l} \rangle_0$, as $U \rightarrow 0$. On the other hand, using the large U asymptotic formulae for $\lim_{L \rightarrow \infty} \tau_0(l)$ (see Appendix B), we obtain: for $U \rightarrow \infty$

$$\lim_{L \rightarrow \infty} \langle a_x^+ a_{x+l} \rangle_1 \approx \begin{cases} (\pi \alpha (l+1))^{-1} \sin \pi \rho_e (l+1) \\ + (\pi \alpha (l-1))^{-1} \sin \pi \rho_e (l-1), & l = 2s + 1, \quad s = 0, 1, \dots, \\ (1 + (-1)^x) (\pi l)^{-1} \sin \pi \rho_e l, & l = 2s, \quad s = 1, 2, \dots \end{cases} \quad (79)$$

In particular, for $\rho_e = 1/2$, $\lim_{U \rightarrow \infty} \lim_{L \rightarrow \infty} \langle a_x^+ a_{x+l} \rangle_1 \equiv 0$. From now on, we consider only the case of $\rho_e = 1/2$. In the infinite-chain limit, $\lim_{L \rightarrow \infty} \langle a_x^+ a_{x+2s} \rangle_0 = 0$, $s = 1, 2, \dots$, thus

$$\lim_{L \rightarrow \infty} \langle a_x^+ a_{x+l} \rangle_1 = \begin{cases} \lim_{L \rightarrow \infty} \tau_1(l), & l = 2s + 1, \quad s = 0, 1, \dots, \\ (-1)^x \alpha \lim_{L \rightarrow \infty} \tau_0(l), & l = 2s, \quad s = 1, 2, \dots \end{cases} \quad (80)$$

By [28] (see also Appendix B),

$$\begin{aligned}\lim_{L \rightarrow \infty} \tau_0(2s) &= \frac{\kappa}{4\pi} \int_0^\pi \frac{\cos(2sk)}{\sqrt{1 - \kappa^2 \sin^2 k}} dk = (-1)^s \frac{\kappa}{4\pi} \int_0^\pi \frac{\cos(2sk)}{\sqrt{1 - \kappa^2 \cos^2 k}} dk \\ &= (-1)^s \frac{\kappa^{2s+1}}{2^{3s+2}} \frac{(2s-1)!!}{s!} F\left(s + \frac{1}{2}, s + \frac{1}{2}, 2s + 1; \kappa^2\right),\end{aligned}\quad (81)$$

and

$$\begin{aligned}\lim_{L \rightarrow \infty} \tau_1(2s+1) &= (-1)^s \frac{\kappa^{2s+1}}{2^{3s+2}} \frac{(2s-1)!!}{s!} \left\{ F\left(s + \frac{1}{2}, s + \frac{1}{2}, 2s + 1; \kappa^2\right) \right. \\ &\quad \left. - \frac{\kappa^2}{2^3} \frac{2s+1}{s+1} F\left(s + \frac{3}{2}, s + \frac{3}{2}, 2s + 3; \kappa^2\right) \right\},\end{aligned}\quad (82)$$

where $F(a, b, c; z)$ stands for the hypergeometric function [27, 29]. By means of an integral representation of $F(a, b, c; z)$ [29], $\tau_0(2s)$ can be rewritten in the following form

$$\lim_{L \rightarrow \infty} \tau_0(2s) = (-1)^s \frac{\kappa^{2s+1}}{4\pi} \int_0^1 \exp\left[s \ln \frac{t(1-t)}{1 - \kappa^2 t}\right] \frac{dt}{\sqrt{t(1-t)(1 - \kappa^2 t)}},\quad (83)$$

which is suitable for determining the asymptotics of $\tau_0(2s)$ for $s \rightarrow \infty$. Using the Laplace asymptotic formula [30] for the integral in (83), we obtain

$$\lim_{L \rightarrow \infty} \tau_0(2s) \approx (-1)^s \frac{1}{4\sqrt{\pi}} \frac{1}{\sqrt[4]{(\frac{U}{4})^2(1 + (\frac{U}{4})^2)}} \frac{\exp(-s/\xi)}{\sqrt{s}},\quad (84)$$

where the *correlation length* ξ is defined by

$$\xi \equiv -\frac{1}{2 \ln \left(\sqrt{1 + (\frac{U}{4})^2} - \sqrt{(\frac{U}{4})^2} \right)},\quad (85)$$

and has the following asymptotic behaviour:

$$\xi \approx \frac{2}{U}, \quad \text{for } U \rightarrow 0,\quad (86)$$

and

$$\xi \approx \frac{1}{2 \ln(\frac{U}{2})}, \quad \text{for } U \rightarrow \infty.\quad (87)$$

In Fig. 2 we show ξ as a function of U , obtained from the exact formula (85) and from fitting numerically calculated correlation function $\langle a_x^+ a_{x+2s} \rangle_1$ with the formula $const \exp(-s/\xi)$. We plot also in Fig. 2 the asymptotic formulae (86) and (87). As a matter of fact, the formula (86) approximates the exact value of ξ with accuracy 10^{-2} , up to $U = 1$. The formula (87) approximates ξ with accuracy $2,5 \cdot 10^{-2}$, for $U \geq 10$. Consequently, we find the asymptotic forms of the two-point function $\langle a_x^+ a_{x+l} \rangle_1$:

$$l = 2s, \quad |\langle a_x^+ a_{x+2s} \rangle_1|^2 \approx \frac{1}{2\pi} \frac{\frac{U}{4}}{\sqrt{1 + (\frac{U}{4})^2}} \frac{\exp(-2s/\xi)}{2s},\quad (88)$$

and

$$l = 2s + 1, \quad |\langle a_x^+ a_{x+2s+1} \rangle_1|^2 \approx \frac{1}{8\pi} \frac{1}{\sqrt{(\frac{U}{4})^2(1 + (\frac{U}{4})^2)}} \left[1 - \frac{\exp(-1/\xi)}{\sqrt{1 + 1/s}} \right]^2 \frac{\exp(-2s/\xi)}{2s}. \quad (89)$$

Having obtained the correlation functions $\langle n_x \rangle_1$ and $\langle a_x^+ a_{x+l} \rangle_1$, we can easily calculate other correlations of interest. The short-range correlation functions (22), (23), for $l = 0$ read:

$$\mathcal{L}_p(0) = \rho_e(1 - \rho_e), \quad (90)$$

$$\mathcal{S}_p(0) = \frac{1}{2} - \alpha\tau_0(0). \quad (91)$$

Then, for $l > 0$ and any $\rho_e \leq 1/2$ we find

$$\mathcal{L}_p(l) = (-1)^l \alpha^2 \tau_0^2(0) - \begin{cases} \tau_1^2(l), & l = 2s + 1, \quad s = 0, 1, \dots, \\ \langle a_x^+ a_{x+l} \rangle_0^2 + \alpha^2 \tau_0^2(l), & l = 2s, \quad s = 1, 2, \dots, \end{cases} \quad (92)$$

$$\begin{aligned} & \mathcal{S}_p(l) = \left(\rho_e - \frac{1}{2}\right)^2 \\ & + (-1)^l \left[\frac{1}{2} - \alpha\tau_0(0) \right]^2 - \begin{cases} \tau_1^2(l), & l = 2s + 1, \quad s = 0, 1, \dots, \\ \langle a_x^+ a_{x+l} \rangle_0^2 + \alpha^2 \tau_0^2(l), & l = 2s, \quad s = 1, 2, \dots \end{cases} \end{aligned} \quad (93)$$

In the infinite-chain limit and for $\rho_e = 1/2$, the above short-range correlation functions assume the form:

$$\begin{aligned} \mathcal{L}(l) &= \lim_{L \rightarrow \infty} \mathcal{L}_p(l) \\ &= (-1)^l \alpha^2 \lim_{L \rightarrow \infty} \tau_0^2(0) - \begin{cases} \lim_{L \rightarrow \infty} \tau_1^2(l), & l = 2s + 1, \quad s = 0, 1, \dots, \\ \alpha^2 \lim_{L \rightarrow \infty} \tau_0^2(l), & l = 2s, \quad s = 1, 2, \dots, \end{cases} \end{aligned} \quad (94)$$

$$\begin{aligned} & \mathcal{S}(l) = \lim_{L \rightarrow \infty} \mathcal{S}_p(l) \\ &= (-1)^l \left[\frac{1}{2} - \alpha \lim_{L \rightarrow \infty} \tau_0(0) \right]^2 - \begin{cases} \lim_{L \rightarrow \infty} \tau_1^2(l), & l = 2s + 1, \quad s = 0, 1, \dots, \\ \alpha^2 \lim_{L \rightarrow \infty} \tau_0^2(l), & l = 2s, \quad s = 1, 2, \dots \end{cases} \end{aligned} \quad (95)$$

The short-range correlations, given by (94) and (95), are shown in Fig. 3 as functions of the distance, and in Fig. 4 as functions of U . As U increases, the absolute value of \mathcal{L} increases, while the absolute value of \mathcal{S} decreases. At distance $l = 1$, a minimum, known as the correlation hole [25], is clearly visible. Then, at distances greater than a few lattice constants, the short-range correlations become periodic, due to the exponential decay of the two-point function $\langle a_x^+ a_{x+l} \rangle_1$. Using (43), (44), and (45), we easily find the infinite-chain long-range correlation functions $\mathcal{P}(\pi)$, \mathcal{L} , and \mathcal{S} . For $\rho_e = 1/2$ they read:

$$\mathcal{P}(\pi) = \lim_{L \rightarrow \infty} \mathcal{P}_p(\pi) = \alpha^2 \lim_{L \rightarrow \infty} \tau_0^2(0), \quad (96)$$

$$\mathcal{L} = \lim_{L \rightarrow \infty} \mathcal{L}_p = \frac{1}{4} \alpha^2 \lim_{L \rightarrow \infty} \tau_0^2(0), \quad (97)$$

$$\mathcal{S} = \frac{1}{16} \left(1 - 2\alpha \lim_{L \rightarrow \infty} \tau_0(0) \right)^2. \quad (98)$$

For checkerboard configurations, $\mathcal{P}(\pi)$ and \mathcal{L} are proportional. Using the asymptotic formulae of Appendix B, we find that as $U \rightarrow \infty$, $\mathcal{P}(\pi) \rightarrow 1/4$, $\mathcal{L} \rightarrow 1/16$, and $\mathcal{S} \rightarrow 0$. The variation of long-range correlations versus U is shown in Fig. 5. As U increases, the quantum fluctuations decrease, but rather slowly, disappearing only in the limit of infinite U . For $U = 5$, \mathcal{L} attains 77% of its saturation value, and for $U = 8.3$, 90% of it.

5 Correlation functions – numerical results

In the previous section we have been able to determine analytically the spatial and U dependence of a number of correlation functions, in the case of $G = [1/2]$. Here, our aim is to present the spatial and U dependence of the same kind of correlation functions, but with other choices of the set G . Specifically, we consider the following sets of low-period ground-state configurations: $[1/6]_1$, $[1/6]_2$, $[1/6]_3$, $[1/3]$, $[2/5]$, $[3/7]$, $[1/4]_2$; atomic, 2-molecular and 3-molecular configurations are included in the list. The corresponding stability intervals of U , determined approximately by means of restricted ground-state phase diagrams obtained in [13], read: $\Delta U_{[1/6]_1} = [0.6, \infty)$, $\Delta U_{[1/6]_2} = [0.3, 2.7]$, $\Delta U_{[1/6]_3} = [0.1, 1.0]$, $\Delta U_{[1/3]_1} = [0.2, \infty)$, $\Delta U_{[2/5]_1} = [0.1, \infty)$, $\Delta U_{[3/7]_1} = [0.05, \infty)$, $\Delta U_{[1/4]_2} = [0.3, 2.2]$. In contradistinction to the previous section, the results reported here have been obtained numerically. We have used numerical procedures elaborated for a study of spin chains [31], with the main part being an exact diagonalization of the matrix $\langle x|h_b(w)|y\rangle$, defined by (46), (47). The size of the chains has varied from a few hundred up to a few thousand sites. In the calculations, we have imposed the free boundary conditions on a chain whose number of sites, L , was chosen in such a way that L was a multiple of $4q$, with q being the period of the configurations in G under consideration. The one-point, broken symmetry averages $\langle n_x \rangle_{b,g}$, and the two-point, symmetric, short-range correlations, $\mathcal{L}_{b,x}(l)$ and $\mathcal{S}_{b,x}(l)$, have been calculated using the formulae (53). To weaken the effect of the chain ends, the site x and distance l have been chosen so that all the sites involved in the calculations of correlations were well inside the chain. The results obtained for chains of different sizes have been extrapolated to the infinite-chain limit. Practically, it has appeared that the results obtained for chains of $L = 420$ coincided with the corresponding infinite-chain results with accuracy (the relative error) exceeding 10^{-12} .

In Figs. 6, 7, 8, we show short-range correlations as functions of distance. All the plots of two-point correlation functions, versus distance, exhibit a minimum at distance one, i.e. the so called correlation hole [25], and after a few further steps become perfectly periodic, because of the exponential decay of the function $\langle a_x^+ a_{x+l} \rangle$ (see below). In Figs. 9 – 12 we have plotted the short-range correlations, for a few small distances, as functions of U . Typically, in the presented cases the short-range correlations vary monotonically with U . However, $\mathcal{S}(1)$ for $G = [1/6]_1$ (shown in Fig. 12) exhibits a minimum for some $U < 1$. It is caused by a non-monotonic behaviour of $\langle n_x \rangle_g$ at nearest neighbours of the occupied site; for small U ($U < 0.5$ roughly) it increases, and then decreases (see Fig. 13). We note also that, as $U \rightarrow \infty$, $\mathcal{S}(0)$, $\mathcal{S}(1)$ do not tend to 0, for molecular configurations. This is the case also for $\mathcal{S}(2)$ in the case of 3-molecular configurations $[1/6]_3$. The reason is that for molecular configurations, the local density of electrons at site x does not tend to g_x as $U \rightarrow \infty$, but obeys, for molecules greater than 3-molecules, some nontrivial distribution. This is shown in Fig. 13.

Of particular interest is the spatial decay of the two-point correlation function $|\langle a_x^+ a_{x+l} \rangle_b|^2$. The exact calculations carried out for checkerboard configurations, in the previous section, suggest that for periodic ion configurations this decay is of the form $l^{-\gamma} \exp(-l/\xi)$, with some positive γ . Thus, this decay can be characterized by the correlation length ξ and the index γ . Specifically, for checkerboard configurations we have obtained ξ as a function of U (85), with $\xi^{-1} = U/2$, for small U , that is ξ^{-1} amounts to a half of the gap at the Fermi level, and with $\gamma = 1$, according to (88), (89). For G other than the checkerboard configurations, we have approximated the large distance behaviour of $|\langle a_x^+ a_{x+l} \rangle_b|^2$ by the formula $const \exp(-l/\xi)$, thus ignoring the possible power-law prefactor $l^{-\gamma}$. The data are shown in Fig. 14. Comparing the data obtained in such calculations of ξ with the exact results in the case of the checkerboard configurations, we estimate the error to be at the level of a few per cent. To reach such an accuracy, in the range of $U < 0.4$ it was necessary to consider a chain with $L = 2 \cdot 10^3$, while

for larger U it was enough to take $L = 10^3$. For all the studied periodic configurations, we have found that for small U the inverse correlation length $\xi^{-1} \approx \text{const}\Delta$, with Δ being the gap at the Fermi level, and $\Delta \sim U$.

Finally we present our results concerned with the defined in Section 3 long-range correlation functions. Our purpose was not only to calculate the correlations $\mathcal{P}_f(k)$, \mathcal{L}_f , and \mathcal{S}_f , in the infinite-chain limit, but also to observe their dependence on the chain size L , in a finite chain with the free boundary conditions imposed ($b = f$). To calculate the long-range correlations, we used their definitions (31), (32), (33), which involve all sites of the chain, and the simplified expressions, involving $L/2$ central sites of the chain,

$$\mathcal{P}'_f(k) = \frac{2}{L} \sum_{l=0}^{L/2-1} e^{-ikl} \mathcal{L}_{f,x}(l), \quad (99)$$

$$\mathcal{L}'_f = \frac{2}{L} \sum_{l=0}^{L/2-1} E_p(l) \mathcal{L}_{f,x}(l), \quad (100)$$

$$\mathcal{S}'_f = \frac{2}{L} \sum_{l=0}^{L/2-1} E_p(l) \mathcal{S}_{f,x}(l), \quad (101)$$

where $x = L/4$. As shown in Fig. 15, for particular sets G and values of U , the long-range correlations vary linearly with $1/L$, and the simplified expressions, being less sensitive to the boundaries of the chain, for given L constitute a lot better approximation to the infinite-chain value of correlations than the defining formulae. The dependence of infinite-chain values of \mathcal{P} , \mathcal{L} , and \mathcal{S} on U , for different choices of the set G , is displayed in Figs. 16, 17. As a rule, \mathcal{L} increases towards a positive saturation value, while \mathcal{S} decreases towards zero, for all the considered sets G , except $G = [1/6]_3$, when \mathcal{S} exhibits a minimum at $U \approx 2$. For $U > 2$, \mathcal{S} increases towards a positive asymptote. An inspection of the local density of electrons, as a function U , reveals a non-monotonic behaviour of this density at nearest neighbours of the central occupied site of the 3-molecule: it has the maximum at $U \approx 2$ and decreases towards a positive asymptote, as $U \rightarrow \infty$ (see Fig. 13). Therefore, the non-monotonic behaviour of the local density is responsible for the non-monotonic behaviour of \mathcal{S} .

6 Summary and discussion

In the paper, we have studied analytically and numerically, the spatial and U dependence of short-range and long-range ground-state correlation functions of electrons in the Falicov-Kimball chain. We have chosen the electron-ion coupling $U > 0$, which amounts, in our case, to attraction between the electrons and ions. The obtained results can be transformed to the case of repulsion by means of hole-particle transformations [2]. We emphasize also that only nearest-neighbour, uncorrelated with ions, hopping of electrons has been taken into account. The properties of electron correlations in the case of extended or correlated with ions hopping will be presented elsewhere. The calculations have been carried out in different ground states, specified by the sets G of periodic ground-state ion configurations and the corresponding stability intervals ΔU_G . Typically, for a specified G we considered an interval of U having only a non-void intersection with the stability interval of G , ΔU_G .

Outside the stability intervals, the results obtained refer to tight-binding electrons in periodic external potentials, given by G .

We mention that, due to the Jordan-Wigner transformation, our results can also be interpreted in terms of spin-1/2 isotropic XY chains, in periodic transverse external magnetic fields.

It is well known that the two-point correlation function $\langle a_x^+ a_{x+l} \rangle_b$, $l = 0, 1, \dots$, amounts to the one-body reduced density matrix in the ground state. This quantity enables one to calculate ground-state averages of one-body observables [24], and is therefore of crucial importance for all methods that describe many-body systems by means of single-particle formalism, like the density functional theory, for instance. The spatial decay of the one-body reduced density matrix determines the degree of locality of many quantities, which are relevant for describing properties of metals and insulators. For this reason, its asymptotic long-distance behaviour has been the subject of interest for long time. Quite recently, the spatial decay of the one-body reduced density matrix was investigated in some tight-binding models of metals and insulators (see [32], [33], [34], and the references quoted there). In [33] the authors considered a model of an insulator with two-bands separated by a gap, due to two bare electronic states, with different bare energies, at each site, with equal in-band transfer integrals and a weak interband hybridization. The asymptotic long-distance behaviour of the single-particle density matrix has been studied, in dimensions $D = 1, 2$, and 3 . The dependence of the correlation (decay) length on the energy parameters of the model and the existence of the power-law prefactor, of the form $l^{-D/2}$, has been demonstrated. The results obtained in our paper can be viewed as the results referring to models of many-band insulators, where the bands separated by gaps arise due to a periodic spatial modulation of the bare energies. In the case of two-bands (Section 4), we have been able to calculate exactly the correlation functions, and then extract, in particular, the asymptotic long-distance behaviour of the single-particle density matrix. In the considered here case of $D = 1$, we have found the $l^{-1/2}$ prefactor, as in [33], and the exact expression for the correlation length ξ , given by (85), as a function of the periodic-potential strength U (which amounts also to the gap width). For a weak potential, the inverse correlation length $\xi^{-1} \approx U/2$, while for a strong potential, $\xi^{-1} \approx 2 \ln(U/2)$.

In [35], Macêdo et al calculated the correlation function $\mathcal{S}(l)$, given by (95), as the $T \rightarrow 0$ limit of the corresponding grand-canonical correlation function, that is, with the ground-state symmetric average in definition (23) replaced by the grand canonical average. The chemical potential was chosen in such a way that the ground-state was characterized by the set $[1/2]_1$ of checkerboard ion configurations. In the case of the one-dimensional system under consideration, the grand canonical correlation functions should coincide with the canonical ones. The results in [35] have been obtained using the method of small-cluster exact diagonalization and extrapolation techniques to the infinite chain, where the cluster size was limited to at most 10 sites. To compare the values of $\mathcal{S}(l)$, obtained from the exact formula (95), and those displayed in figures of [35], one has to change the sign of U in (95), and to multiply our $\mathcal{S}(l)$ by $3/4$. The results of exact calculations are shown in Table 1, and they differ qualitatively from the data displayed in [35].

The ground-state phase diagram of the Falicov-Kimball model is rich in quantum phase transitions, that is the phase transitions where the role of thermal fluctuations is played by quantum fluctuations [36]. These transitions are driven by such control parameters as ρ_e , ρ_i , and U . They occur, when for some critical value of a control parameter, the nature of the ground state changes. A detailed description of quantum phase transitions in a many-body, interacting system, like the Falicov-Kimball model, is a hard task (for recent results see [37], [38]). We would like to point out that the analytic results of Section 4, can be used to describe a simple instance of a quantum phase transition, driven by U , with the critical value $U_c = 0$. Consider an

Table 1: $3\mathcal{S}(l)/4$

l	$U = 0$	$U = -4$	$U = -8$
0	0.375	0.688	0.729
1	-0.236	-0.658	-0.719
2	0.188	0.630	0.710
3	-0.196	-0.632	-0.710

infinite chain, whose particle densities are set to $1/2$, $\rho_i = \rho_e = 1/2$. Obviously, as $U = U_c = 0$ there is no order in the ion subsystem, whereas the electrons are distributed uniformly. There is no gap in the electron energy spectrum and the truncated electron density-density correlation function, $\langle n_x n_{x+l} \rangle - 1/4$, exhibits a power-law decay l^{-2} (with the oscillations owing to $\sin^2(\pi l/2)$ imposed) as $l \rightarrow \infty$, according to (59). On the other hand, for an arbitrary nonzero U , the ion subsystem becomes checkerboard ordered [4, 5]. The electrons follow the periodic distribution of the ions, for instance the broken-symmetry average $\langle n_x \rangle_1$ is modulated with period 2 (67). A gap $\Delta = U$ appears at the Fermi level, and correspondingly, the large-distance behaviour of the broken-average truncated density-density correlation function, $\langle n_x n_{x+l} \rangle_1 - \langle n_x \rangle_1 \langle n_{x+l} \rangle_1$, changes to an exponential one, of the form $l^{-1} \exp(-l/\xi)$ (see (88), (89)), with the correlation length $\xi \sim U^{-1}$, which diverges as $U \rightarrow 0$.

Acknowledgements

T. K. is grateful to the University of Wrocław for a kind hospitality during the completion of this manuscript.

7 Appendix A

Here we define the short- and long-range correlation functions for the ion subsystem. For any ion configuration $g \in G$, and its restriction to a finite chain whose number of sites, L , is a multiple of the period q of the ground-state configurations g ,

$$q^{-1} \sum_{g \in G} g_x = \rho_i = L^{-1} \sum_{x=0}^{L-1} g_x. \quad (102)$$

The *short-range ion-ion correlation function* is

$$E_{b,x}(l) = q^{-1} \sum_{g \in G} (g_x - \rho_i) (g_{x+l} - \rho_i), \quad (103)$$

which for $b = p$ is translation invariant. The degree of order can be "measured" either by the *ion-order parameter*, $I_{b,g}(k)$, which for given $g \in G$ and $k = 2\pi\rho_e = 2\pi p/q$ is

$$I_{b,g}(k) = L^{-1} \sum_{x=0}^{L-1} e^{ikx} (g_x - \rho_i); \quad \sum_g I_{b,g}(k) \equiv 0, \quad (104)$$

or by the long-range correlation, $q^{-1} \sum_{g \in G} |I_{b,g}(k)|^2$,

$$q^{-1} \sum_{g \in G} |I_{b,g}(k)|^2 = L^{-2} \sum_{x,y=0}^{L-1} e^{ik(x-y)} q^{-1} \sum_{g \in G} [(g_x - \rho_i) (g_y - \rho_i)]. \quad (105)$$

The function $k \rightarrow q^{-1} \sum_{g \in G} |I_{b,g}(k)|^2$ is the static structure factor for the ions. For periodic boundary conditions,

$$q^{-1} \sum_{g \in G} |I_{p,g}(k)|^2 = |I_{p,g}(k)|^2 = q^{-2} \sum_{x,y=0}^{q-1} e^{ik(x-y)} (g_x - \rho_i) (g_y - \rho_i) > 0, \quad (106)$$

where the above inequality follows from the argument presented in the Appendix of [8]. Thus, the square of the absolute value of the ion-order parameter is a measure of the ion-ion long-range order.

8 Appendix B

For $\rho_e < 1/2$, the large U asymptotic behaviour of $\lim_{L \rightarrow \infty} \tau_0(l)$ is smooth in ρ_e and reads:

$$\begin{aligned} \text{for } U \rightarrow \infty, \quad \lim_{L \rightarrow \infty} \tau_0(l) \approx & \frac{1}{\pi\alpha} \left\{ \frac{\sin(\pi\rho_e l)}{l} \right. \\ & + \frac{1}{2\alpha^2} \left[2 \frac{\sin(\pi\rho_e l)}{l} - \frac{\sin(\pi\rho_e(l+2))}{l+2} - \frac{\sin(\pi\rho_e(l-2))}{l-2} \right] \\ & + \frac{3}{2\alpha^4} \left[3 \frac{\sin(\pi\rho_e l)}{l} - \frac{5}{2} \left(\frac{\sin(\pi\rho_e(l+2))}{l+2} + \frac{\sin(\pi\rho_e(l-2))}{l-2} \right) \right. \\ & \left. \left. + \frac{\sin(\pi\rho_e(l+4))}{l+4} + \frac{\sin(\pi\rho_e(l-4))}{l-4} \right] \right\}. \end{aligned} \quad (107)$$

In particular,

$$\text{for } U \rightarrow \infty, \quad \lim_{L \rightarrow \infty} \tau_0(0) \approx \rho_e / \alpha. \quad (108)$$

On the other hand, the small U asymptotic behaviour of $\lim_{L \rightarrow \infty} \tau_0(l)$ is singular at $\rho_e = 1/2$. For $\rho_e < 1/2$, the following recursive formula holds:

$$\text{for } U \rightarrow 0, \quad \lim_{L \rightarrow \infty} \tau_0(l) \approx \frac{\sin(\pi\rho_e(l-1))}{\pi(l-1)} - \lim_{L \rightarrow \infty} \tau_0(l-2). \quad (109)$$

Thus, knowing that

$$\text{for } U \rightarrow 0, \quad \lim_{L \rightarrow \infty} \tau_0(0) \approx \frac{1}{2\pi} \ln |\tan[\pi(1+2\rho_e)/4]|, \quad (110)$$

we can obtain the asymptotic formula for any even $l \geq 2$:

$$\begin{aligned} \lim_{L \rightarrow \infty} \tau_0(2n) \approx & \frac{(-1)^n}{2\pi} \left\{ \left[2 \sum_{j=1}^n (-1)^j \frac{\sin(2j-1)\pi\rho_e}{2j-1} + \ln \tan[\pi(1+2\rho_e)/4] \right] \right. \\ & + \frac{\alpha^2}{8} \left[4 \sum_{j=1}^{n-1} (-1)^j (n-j)(n-j+1) \frac{\sin(2j-1)\pi\rho_e}{2j-1} \right. \\ & \left. \left. + (2n^2 - 1/2) \ln \tan[\pi(1+2\rho_e)/4] - \frac{1}{2} \frac{\sin \pi\rho_e}{\cos^2 \pi\rho_e} \right] + \dots \right\}. \end{aligned} \quad (111)$$

Then, for $\rho_e = 1/2$ and $l = 0, 2$ we find:

$$\text{for } U \rightarrow 0, \quad \lim_{L \rightarrow \infty} \tau_0(0) \approx \frac{1}{2\pi} (a_0 + 2 \ln 2 - \ln \alpha), \quad (112)$$

$$\text{for } U \rightarrow 0, \quad \lim_{L \rightarrow \infty} \tau_0(2) \approx \frac{1}{2\pi} (2 - a_0 - 2 \ln 2 + \ln \alpha), \quad (113)$$

with a_0 given by

$$a_0 = \frac{1}{2} \sum_{n=1}^{\infty} \frac{(2n-1)!!}{n(2n)!!} \approx 0.687. \quad (114)$$

9 Appendix C

The relation between the integral in (81) and the hypergeometric function can be obtained as follows:

$$\begin{aligned} \lim_{L \rightarrow \infty} \tau_0(2s) &= \frac{\kappa}{4\pi} \int_0^\pi \frac{\cos(2sk)}{\sqrt{1 - \kappa^2 \sin^2 k}} dk \\ &= \frac{\kappa}{4\pi} \int_0^\pi dk \cos(2sk) \sum_{j=0}^{\infty} \frac{(2j-1)!!}{(2j)!!} \kappa^{2j} \sin^{2j} k \\ &= \frac{\kappa}{4\pi} \sum_{j=0}^{\infty} \frac{(2j-1)!!}{(2j)!!} \kappa^{2j} \int_0^\pi dk \cos(2sk) \sin^{2j} k \\ &= \frac{\kappa}{4\pi} \sum_{j=s}^{\infty} \kappa^{2j} \frac{(2j-1)!!}{(2j)!!} (-1)^s \frac{\pi}{2^{2j}} \frac{(2j)!}{(j+s)!(j-s)!} \\ &= (-1)^s \frac{\kappa}{4} \sum_{j=s}^{\infty} \frac{(2j-1)!!}{(2j)!!} \frac{(2j)!}{(j+s)!(j-s)!} \frac{\kappa^{2j}}{2^{2j}} \\ &= (-1)^s \frac{\kappa}{4} \sum_{j=s}^{\infty} \frac{[(2j-1)!!]^2}{(j+s)!(j-s)!} \frac{\kappa^{2j}}{2^{2j}} \\ &= (-1)^s \frac{\kappa}{4} \sum_{j=0}^{\infty} \frac{[(2s+2j-1)!!]^2}{(2s+j)!} \frac{1}{j!} \frac{\kappa^{2(s+j)}}{2^{2(s+j)}} \\ &= (-1)^s \frac{\kappa^{2s+1}}{4} \sum_{j=0}^{\infty} \frac{\Gamma^2(s + \frac{1}{2} + j)}{\Gamma(2s+1+j)} \frac{\kappa^{2j}}{j!} \\ &= (-1)^s \frac{\kappa^{2s+1}}{4\pi} \frac{\Gamma^2(s + \frac{1}{2})}{\Gamma(2s+1)} F(s + \frac{1}{2}, s + \frac{1}{2}, 2s+1; \kappa^2) \\ &= (-1)^s \frac{\kappa^{2s+1}}{2^{3s+2}} \frac{(2s-1)!!}{s!} F(s + \frac{1}{2}, s + \frac{1}{2}, 2s+1; \kappa^2). \end{aligned} \quad (115)$$

The Laplace asymptotic formula for integrals reads [30]:

$$\int_0^1 f(t) e^{sS(t)} dt \stackrel{s \rightarrow \infty}{\approx} \sqrt{-\frac{2\pi}{sS''(t_0)}} f(t_0) e^{sS(t_0)}, \quad (116)$$

where

$$S(t_0) = \max_t S(t). \quad (117)$$

In the case of the integral in the last line of (83),

$$f(t) \equiv \frac{1}{\sqrt{t(1-t)(1-\kappa^2 t)}}, \quad S(t) \equiv \ln \frac{t(1-t)}{1-\kappa^2 t}, \quad (118)$$

with

$$t_0 = \frac{1 - \sqrt{1 - \kappa^2}}{\kappa^2}, \quad (119)$$

and

$$S(t_0) = \ln(t_0^2) = \ln \left[\frac{1 - \sqrt{1 - \kappa^2}}{\kappa^2} \right]^2, \quad f(t_0) = \frac{\kappa^2}{(1 - \sqrt{1 - \kappa^2})\sqrt{1 - \kappa^2}},$$

$$S''(t_0) = -\frac{2\kappa^4}{\sqrt{1 - \kappa^2}(1 - \sqrt{1 - \kappa^2})^2}. \quad (120)$$

Consequently, the asymptotic form of the considered integral is

$$\sqrt{\frac{\pi}{s}} \frac{1}{\sqrt[4]{1 - \kappa^2}} \left[\frac{1 - \sqrt{1 - \kappa^2}}{\kappa^2} \right]^{2s} = \sqrt{\frac{\pi}{s}} \sqrt[4]{\frac{1 - (\frac{U}{4})^2}{(\frac{U}{4})^2}} e^{-s/\xi}, \quad (121)$$

with ξ given by (85).

References

- [1] L. M. Falicov and J. C. Kimball, *Simple model for semiconductor-metal transitions: SmB₆ and transition-metal oxides*, Phys. Rev. Lett. **22**, 997 (1969)
- [2] C. Gruber and N. Macris, *The Falicov-Kimball model: a review of exact results and extensions*, Hel. Phys. Acta **69**, 850 (1996)
- [3] J. Jędrzejewski and R. Lemański, *Falicov-Kimball models of collective phenomena in solids (A concise guide)*, Acta Physica Polonica B **32**, 3243 (2001)
- [4] U. Brandt and R. Schmidt, *Exact results for the distribution of the f-level ground state occupation in the spinless Falicov-Kimball model*, Z. Phys. B - Condensed Matter **63**, 45 (1986)
- [5] T. Kennedy and E. H. Lieb, *An itinerant electron model with crystalline or magnetic long range order*, Physica A **138**, 320 (1986)
- [6] C. Gruber, *Falicov-Kimball model: a partial review of the ground states problem*, Proceedings of the Marseille's Conference (1999)
- [7] J. K. Freericks, E. H. Lieb, and D. Ueltschi, *Segregation in the Falicov-Kimball model*, Commun. Math. Phys. **227**, 243 (2002) (math-ph/0107003 (2001)); *Phase separation due to quantum mechanical correlations*, Phys. Rev. Lett. **88**, 106401 (2002) (cond-mat/0110251 (2001))
- [8] J. K. Freericks and L. M. Falicov, *Two-state one-dimensional spinless Fermi gas*, Phys. Rev. B **41**, 2163 (1990)

- [9] C. Gruber, J. L. Lebowitz, and N. Macris, *Ground-state configurations of the one-dimensional Falicov-Kimball model*, Phys. Rev. B **48**, 4312 (1993)
- [10] U. Brandt, *Phase separation in the spinless Falicov-Kimball model*, J. Low Temp. Phys. **84**, 477 (1991)
- [11] J. K. Freericks, Ch. Gruber, and N. Macris, *Phase separation in the binary-alloy problem: The one-dimensional spinless Falicov-Kimball model*, Phys. Rev. B **53**, 16189 (1996)
- [12] C. Gruber, D. Ueltschi, and J. Jędrzejewski, *Molecule formation and the Farey tree in the one-dimensional Falicov-Kimball model*, J. Stat. Phys. **76**, 125 (1994)
- [13] Z. Gajek, J. Jędrzejewski, and R. Lemański, *Canonical phase diagrams of the 1D Falicov-Kimball model at $T = 0$* , Physica A **223**, 175 (1996)
- [14] P. Lemberger, *Segregation in the Falicov-Kimball model*, J. Phys. A **25**, 15 (1992)
- [15] Z. Gajek, J. Jędrzejewski, and R. Lemański, *New phases and structural phase transitions in the 1-D Falicov-Kimball model at $T = 0$* , Phase Transitions **57**, 139 (1996)
- [16] S. Gal, *The ground-state phase diagram of the spinless 1D Falicov-Kimball model: numerical studies*, Czechoslovak Journal of Physics **49**, 1105 (1999)
- [17] P. Farkašovský, *Ground-state properties of the Falicov-Kimball model in one and two dimensions*, Eur. Phys. J. B **20**, 209 (2001)
- [18] Z. Gajek and R. Lemański, *Correlated hopping in the 1D Falicov-Kimball model*, Acta Physica Polonica B **32**, 3473 (2001)
- [19] T. Koma and H. Tasaki, *Decay of superconducting and magnetic correlations in one- and two-dimensional Hubbard models*, Phys. Rev. Lett. **68**, 3248 (1992)
- [20] N. Macris and J. Ruiz, *A remark on the decay of superconducting correlations in one- and two-dimensional Hubbard models*, J. Stat. Phys. **75**, 1179 (1994)
- [21] A. Messenger, *The fermionic correlation functions of the Falicov-Kimball model*, Physica A **279**, 408 (2000)
- [22] J. L. Lebowitz and N. Macris, *Low-temperature phases of itinerant fermions interacting with classical phonons: the static Holstein model*, J. Stat. Phys. **76**, 91 (1994)
- [23] J. K. Freericks and V. Zlatić, *Anomalous magnetic response of the spin-one-half Falicov-Kimball model*, Phys. Rev. B **58**, 322 (1998)
- [24] Ph. A. Martin and F. Rothen, *Many-body problems and quantum field theory*, p.120, Springer Verlag, Berlin Heidelberg 2002
- [25] G. D. Mahan, *Many-particle physics*, Plenum Press, New York 1981
- [26] U. Busch and K. A. Penson, *Tight-binding electrons on open chains: Density distribution and correlations*, Phys. Rev. B **36**, 9271 (1987)
- [27] M. Abramowitz and I. A. Stegun, *Handbook of mathematical functions*, National Bureau of Standards, Applied Mathematics Series 55, 1964

- [28] A. P. Prudnikov, Yu. A. Brychkov, and O. I. Marichev, *Integrals and series; elementary functions*, Nauka, Moskva 1981 (in Russian)
- [29] H. Bateman and A. Erdelyi, *Higher transcendental functions*, vol. 1, McGraw-Hill, New York 1953
- [30] C. M. Bender and S. A. Orszag, *Advanced Mathematical methods for Scientists and Engineers I*, Springer, New York 1999
- [31] O. Derzhko and T. Krokhmal'skii, *Numerical approach for the study of the spin- $\frac{1}{2}$ XY chains dynamic properties*, Physica Status Solidi (b) **208**, 221 (1998)
- [32] Sohrab Ismail-Beigi and T. A. Arias, *Locality of the density matrix in metals, semiconductors, and insulators*, Phys. Rev. Lett. **82**, 2127 (1999)
- [33] S. N. Taraskin, D. A. Drabold, and S. R. Elliott, *Spatial decay of the single-particle density matrix in insulators: analytic results in two and three dimensions*, Phys. Rev. Lett. **88**, 196405 (2002)
- [34] S. N. Taraskin, P. A. Fry, X. Zhang, D. A. Drabold, and S. R. Elliott, *Spatial decay of the single-particle density matrix in tight-binding metals: analytic results in two dimensions*, cond-mat/0207443 v2
- [35] C. A. Macêdo, L. G. Azevedo, and A. M. C. de Souza, *Thermodynamics of the one-dimensional half-filled-band Falicov-Kimball model*, Phys. Rev. B **64**, 184441 (2001)
- [36] S. Sachdev, *Quantum phase transitions*, Cambridge University Press, New York 1999
- [37] A. Messenger, *On quantum phase transition. I. Spinless electrons strongly correlated with ions*, J. Stat. Phys. **106**, 723 (2002)
- [38] A. Messenger, *On quantum phase transition. II. The Falicov-Kimball model*, J. Stat. Phys. **106**, 785 (2002)

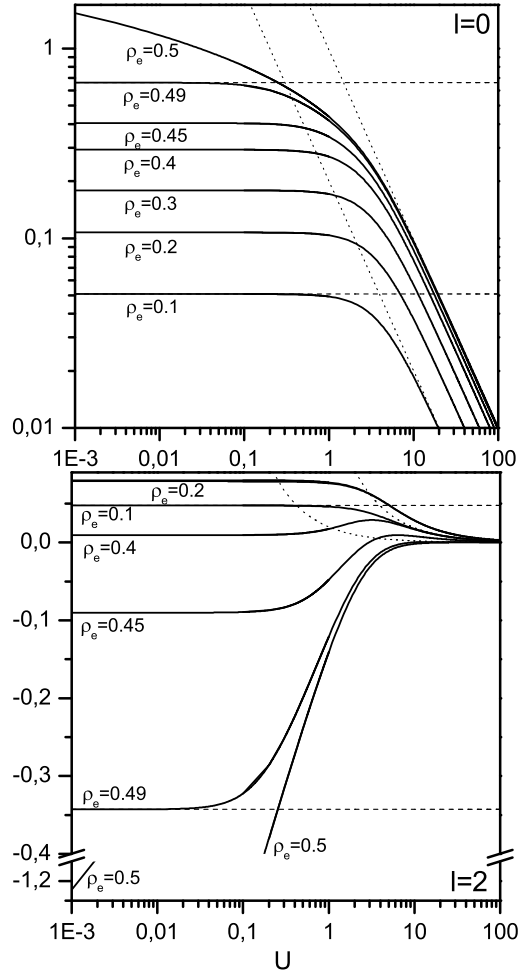


Figure 1: Continuous lines: $\lim_{L \rightarrow \infty} \tau_0(l)$, given by (69), versus U , for $l = 0, 2$ and different values of ρ_e . Dashed lines: the small U asymptotes. Dotted lines: the large U asymptotes.

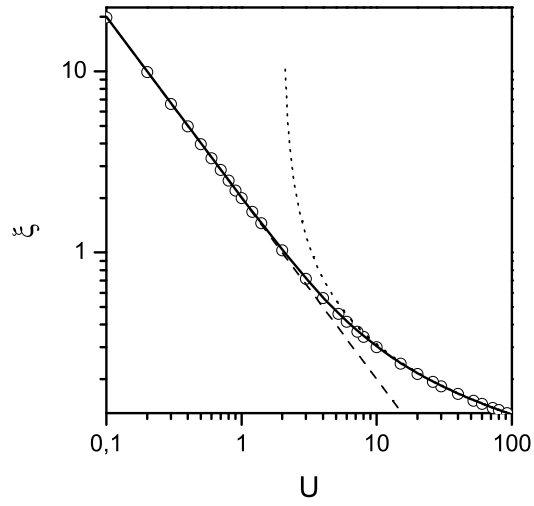


Figure 2: Continuous line: the exact correlation length for the checkerboard configurations, given by (85), versus U . Dashed line: the small U asymptote (86). Dotted line: the large U asymptote (87). Open circles: ξ obtained from fitting numerically calculated correlation function $\langle a_x^+ a_{x+2s} \rangle_1$ with the formula $const \exp(-s/\xi)$.

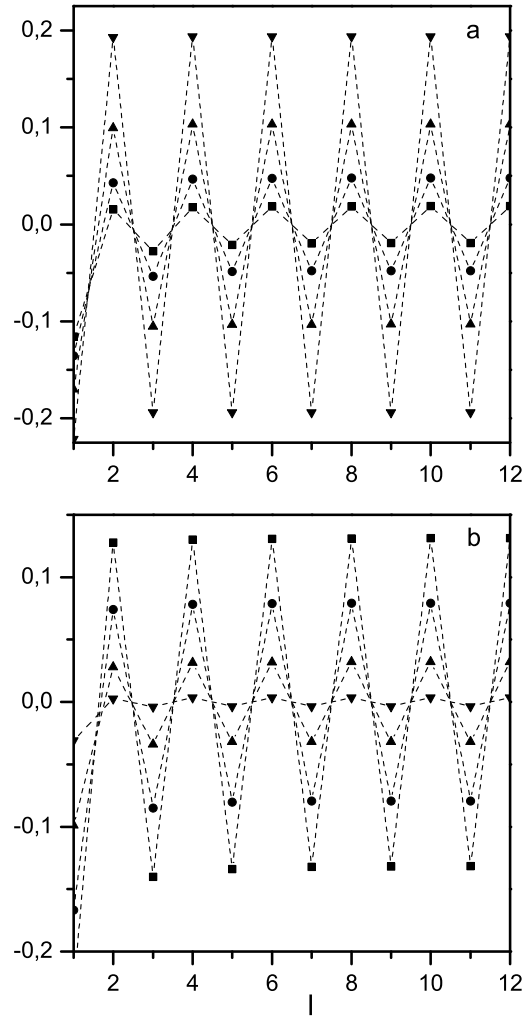


Figure 3: (a) $\mathcal{L}(l)$, given by (94), versus l , for $G = [1/2]_1$, and different values of U . (b) $\mathcal{S}(l)$, given by (95), versus l , for $G = [1/2]_1$, and different values of U . Filled triangles with base up: $U = 5$, filled triangles with base down: $U = 2$, filled circles: $U = 1$, filled squares: $U = 0.5$.

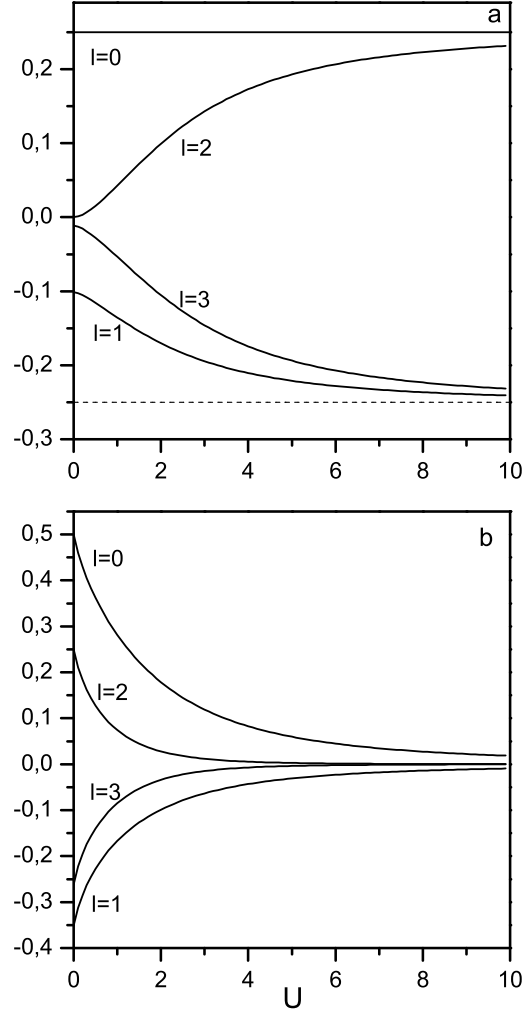


Figure 4: (a) $\mathcal{L}(l)$, given by (94), versus U , for $G = [1/2]_1$, and different values of l . (b) $\mathcal{S}(l)$, given by (95), versus U , for $G = [1/2]_1$, and different values of l . In the scale of the figure, the plots for odd $l \geq 5$ cannot be distinguished from the plot for $l = 3$. Similarly, the plots for $l \geq 4$ cannot be distinguished from the plot for $l = 2$.

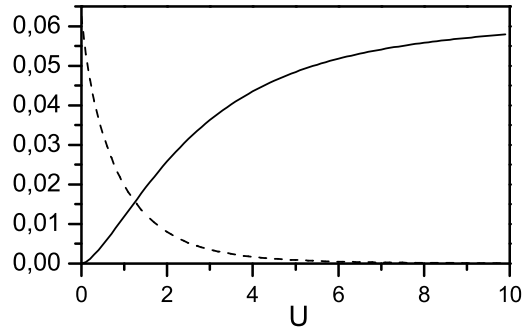


Figure 5: Continuous line: \mathcal{L} for $G = [1/2]_1$, given by (97), versus U . Dashed line: \mathcal{S} for $G = [1/2]_1$, given by (98), versus U .

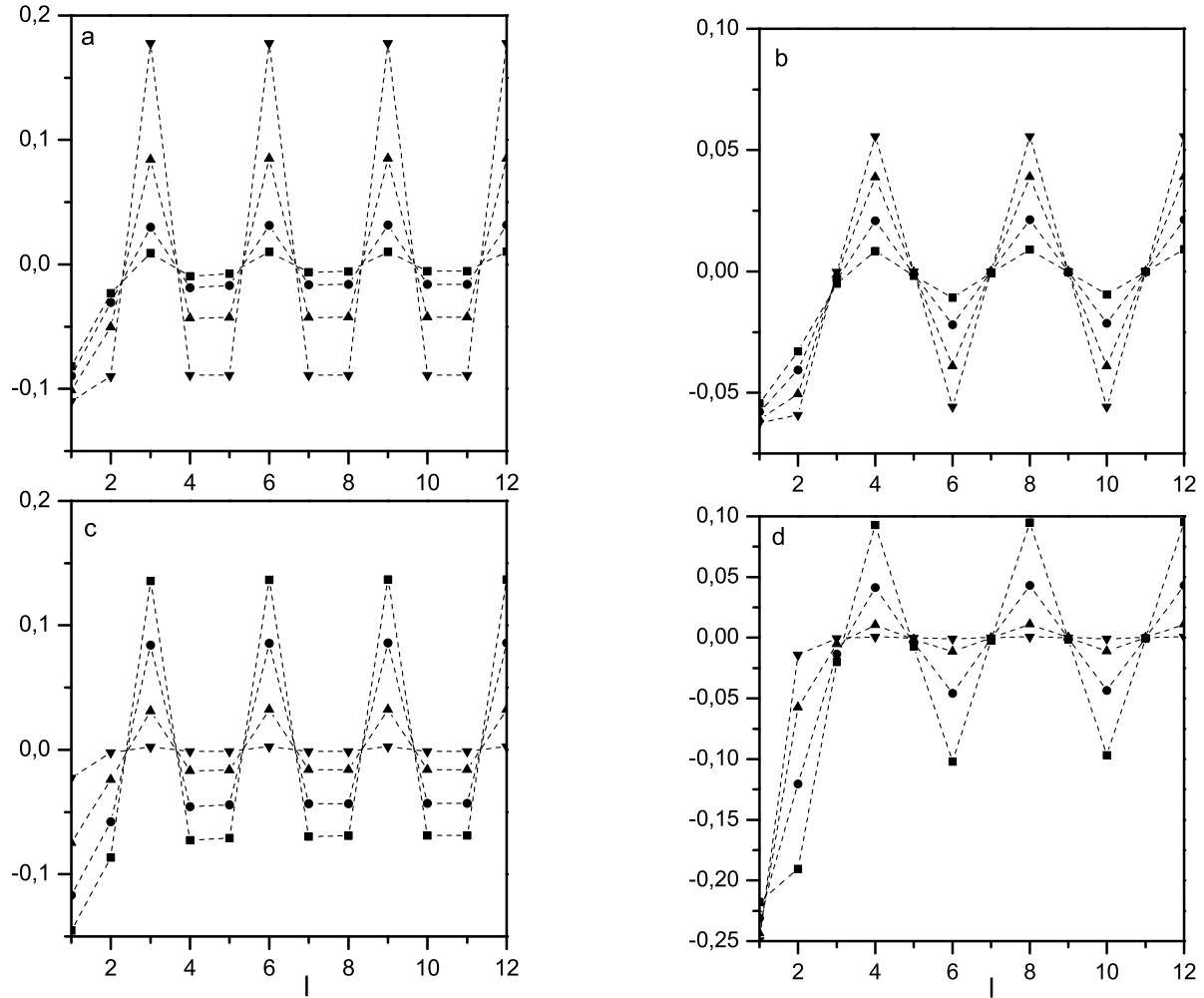


Figure 6: Infinite chain limit of $\mathcal{L}_{f,x}(l)$, given by (22), versus l , for $G = [1/3]_1$ (a), $G = [1/4]_2$ (b), and for different values of U . Infinite chain limit of $\mathcal{S}(l)$, given by (23), versus l , for $G = [1/3]_1$ (c), $G = [1/4]_2$ (d), and different values of U . Filled triangles with base up: $U = 5$, filled triangles with base down: $U = 2$, filled circles: $U = 1$, filled squares: $U = 0.5$.

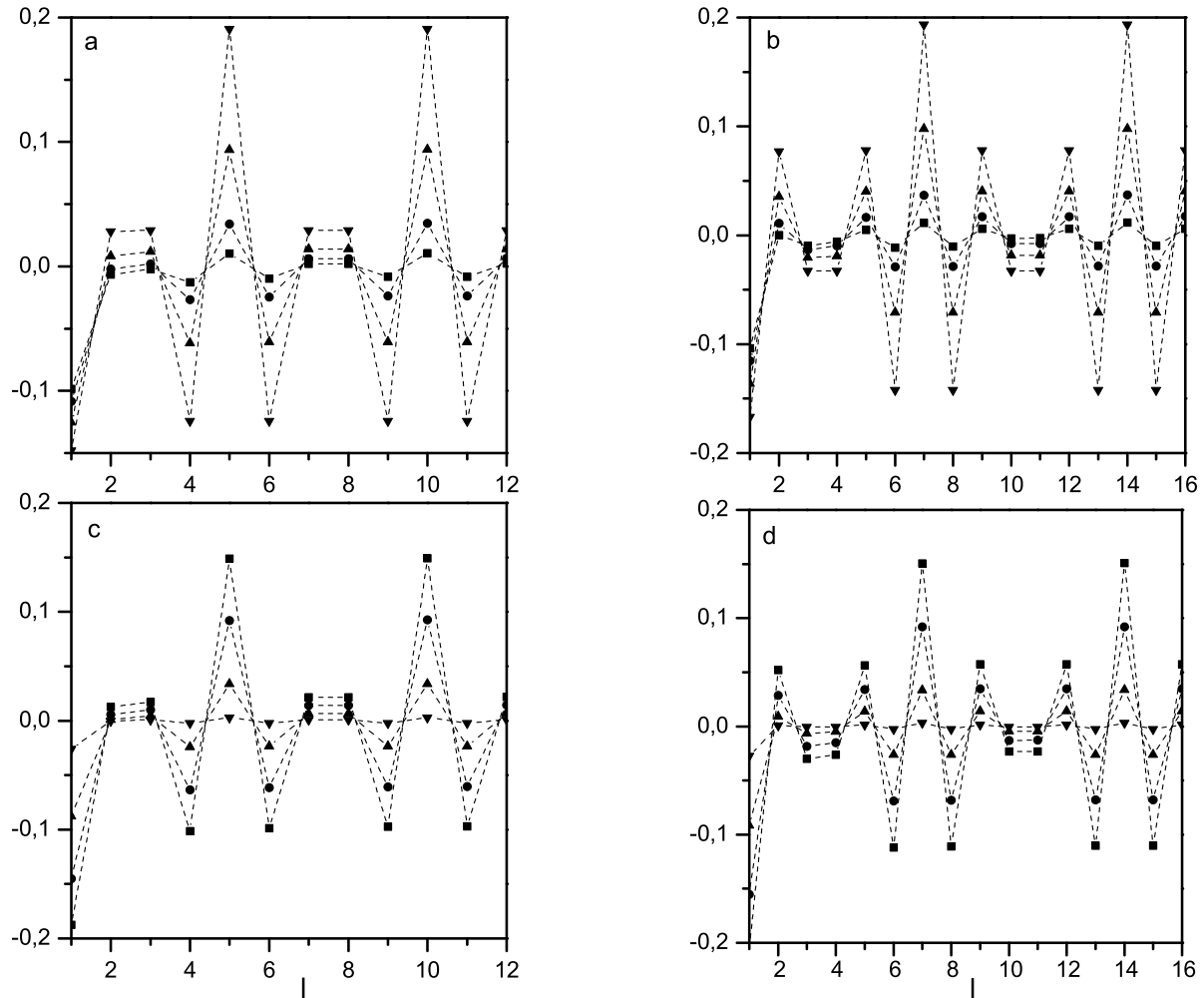


Figure 7: Infinite chain limit of $\mathcal{L}_{f,x}(l)$, given by (22), versus l , for $G = [2/5]_1$ (a), $G = [3/7]_1$ (b), and for different values of U . Infinite chain limit of $\mathcal{S}(l)$, given by (23), versus l , for $G = [2/5]_1$ (c), $G = [3/7]_1$ (d), and different values of U . Filled triangles with base up: $U = 5$, filled triangles with base down: $U = 2$, filled circles: $U = 1$, filled squares: $U = 0.5$.

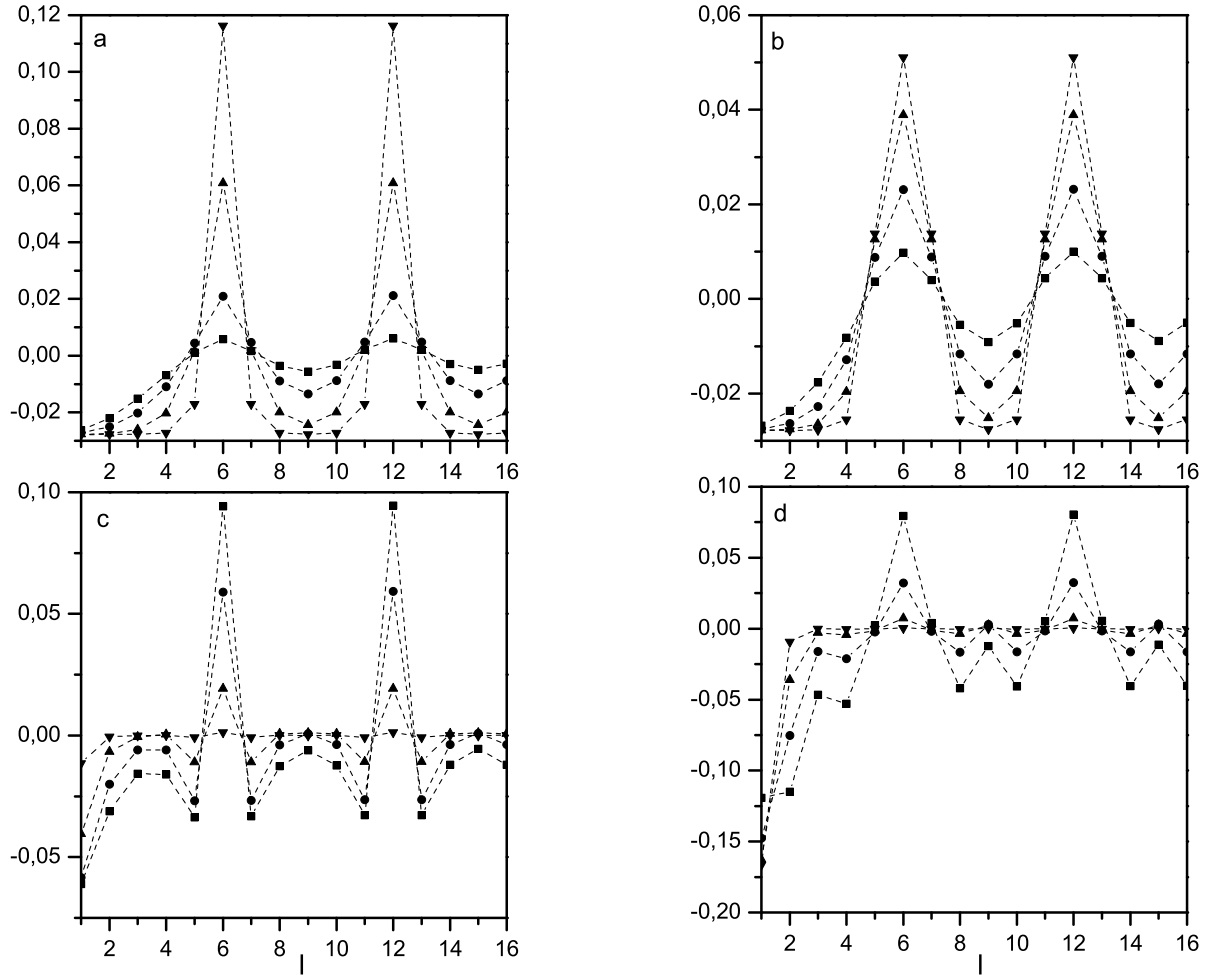


Figure 8: Infinite chain limit of $\mathcal{L}_{f,x}(l)$, given by (22), versus l , for $G = [1/6]_1$ (a), $G = [1/6]_2$ (b), and for different values of U . Infinite chain limit of $\mathcal{S}(l)$, given by (23), versus l , for $G = [1/6]_1$ (c), $G = [1/6]_2$ (d), and different values of U . Filled triangles with base up: $U = 5$, filled triangles with base down: $U = 2$, filled circles: $U = 1$, filled squares: $U = 0.5$.

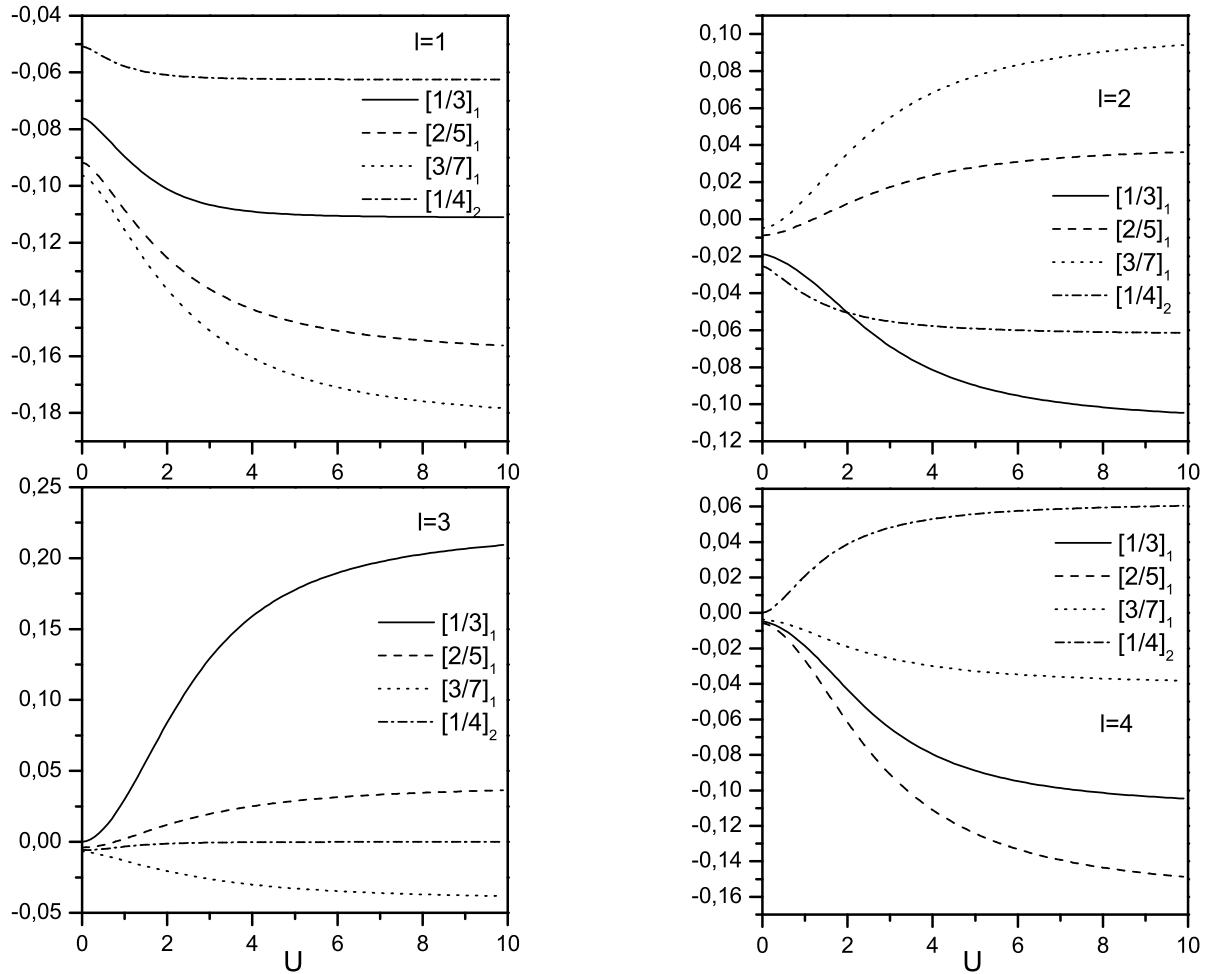


Figure 9: Infinite chain limit of $\mathcal{L}_{f,x}(l)$, given by (22), versus U , for different distances l , and different sets G .

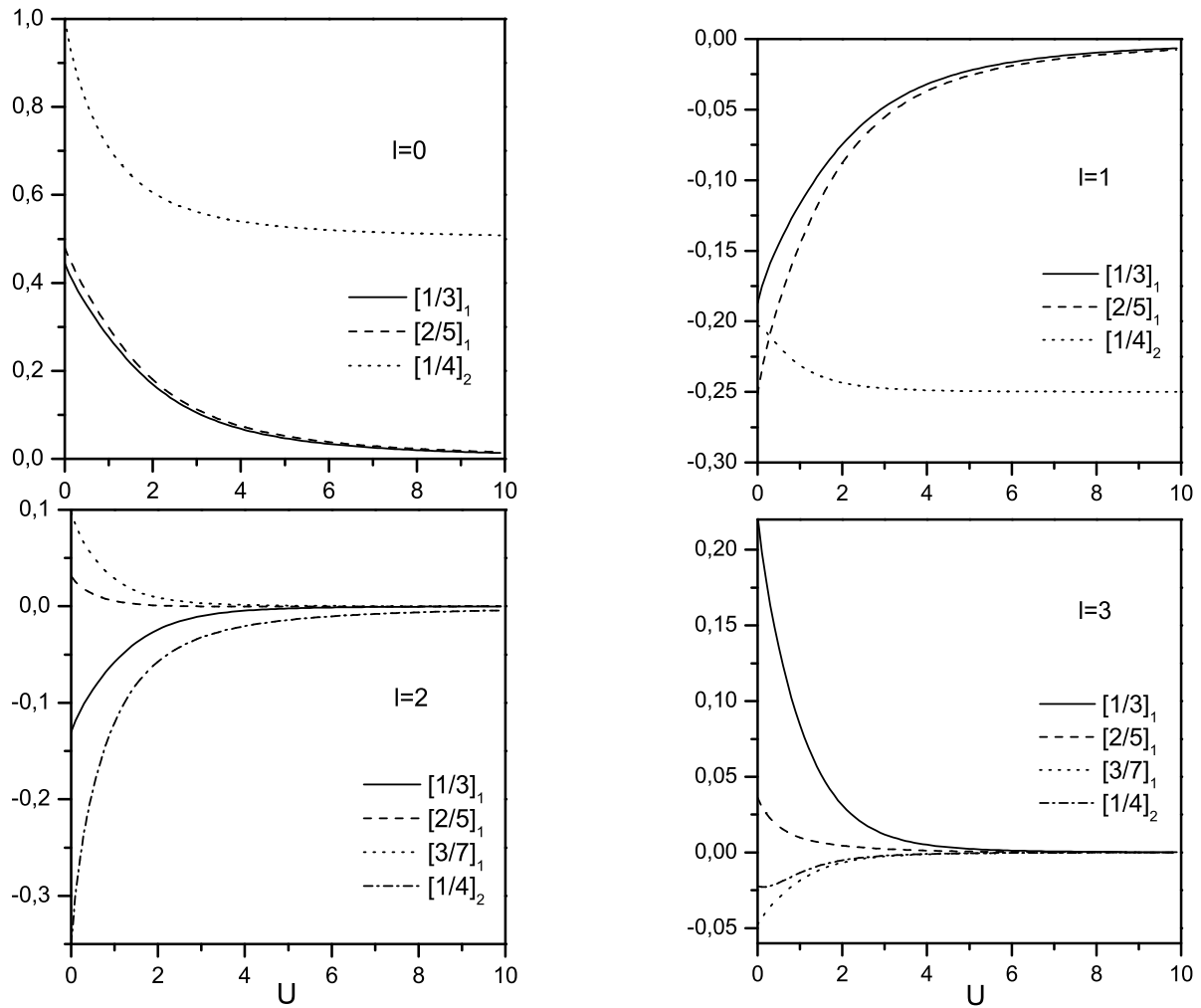


Figure 10: Infinite chain limit of $\mathcal{S}_{f,x}(l)$, given by (23), versus U , for different distances l , and different sets G . Whenever a plot for $G = [3/7]_1$ is missing, it is indistinguishable from the plot for $G = [2/5]_1$, in the scale of the figure.

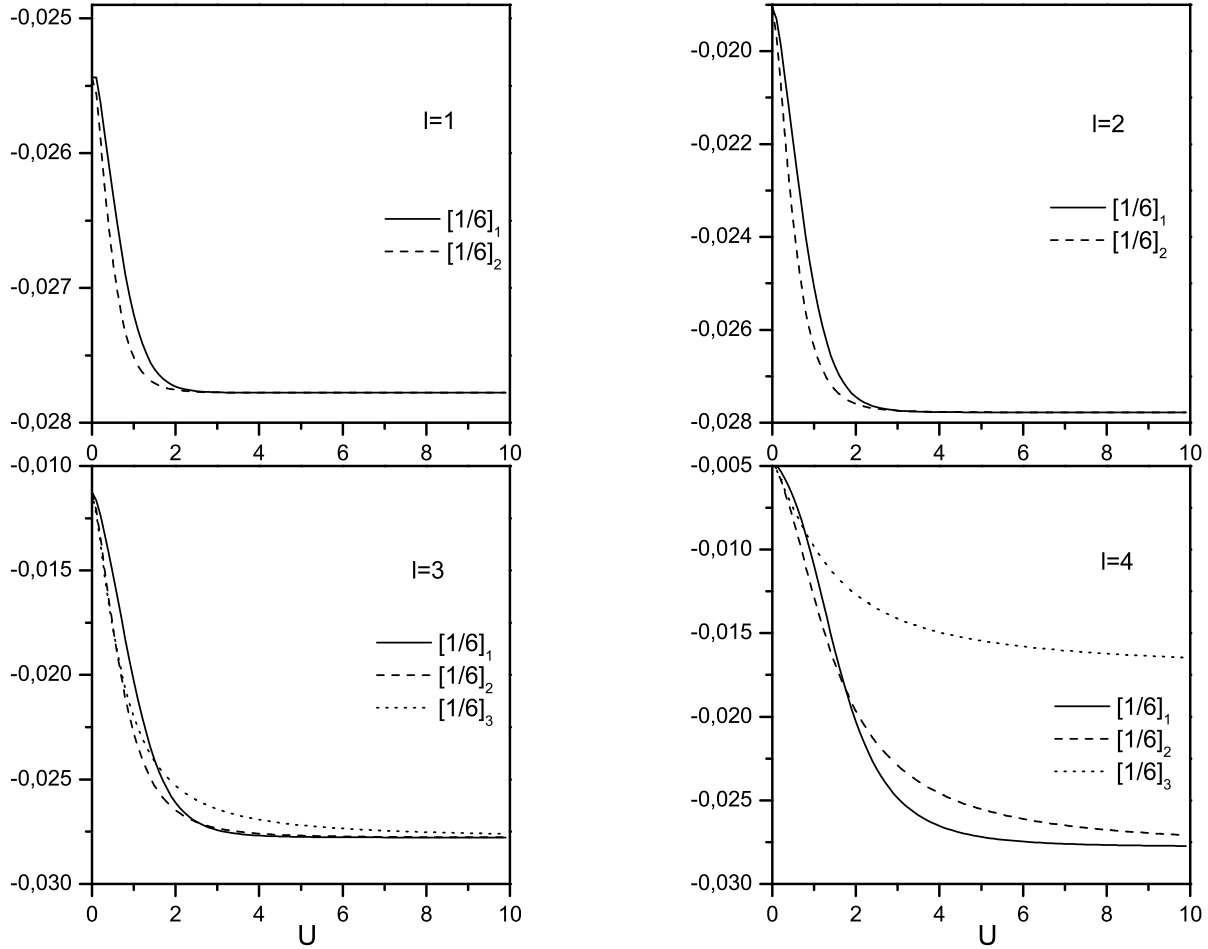


Figure 11: Infinite chain limit of $\mathcal{L}_{f,x}(l)$, given by (22), versus U , for different distances l , and different sets G . Whenever a plot for $G = [1/6]_3$ is missing, it is indistinguishable from the plot for $G = [1/6]_2$, in the scale of the figure.

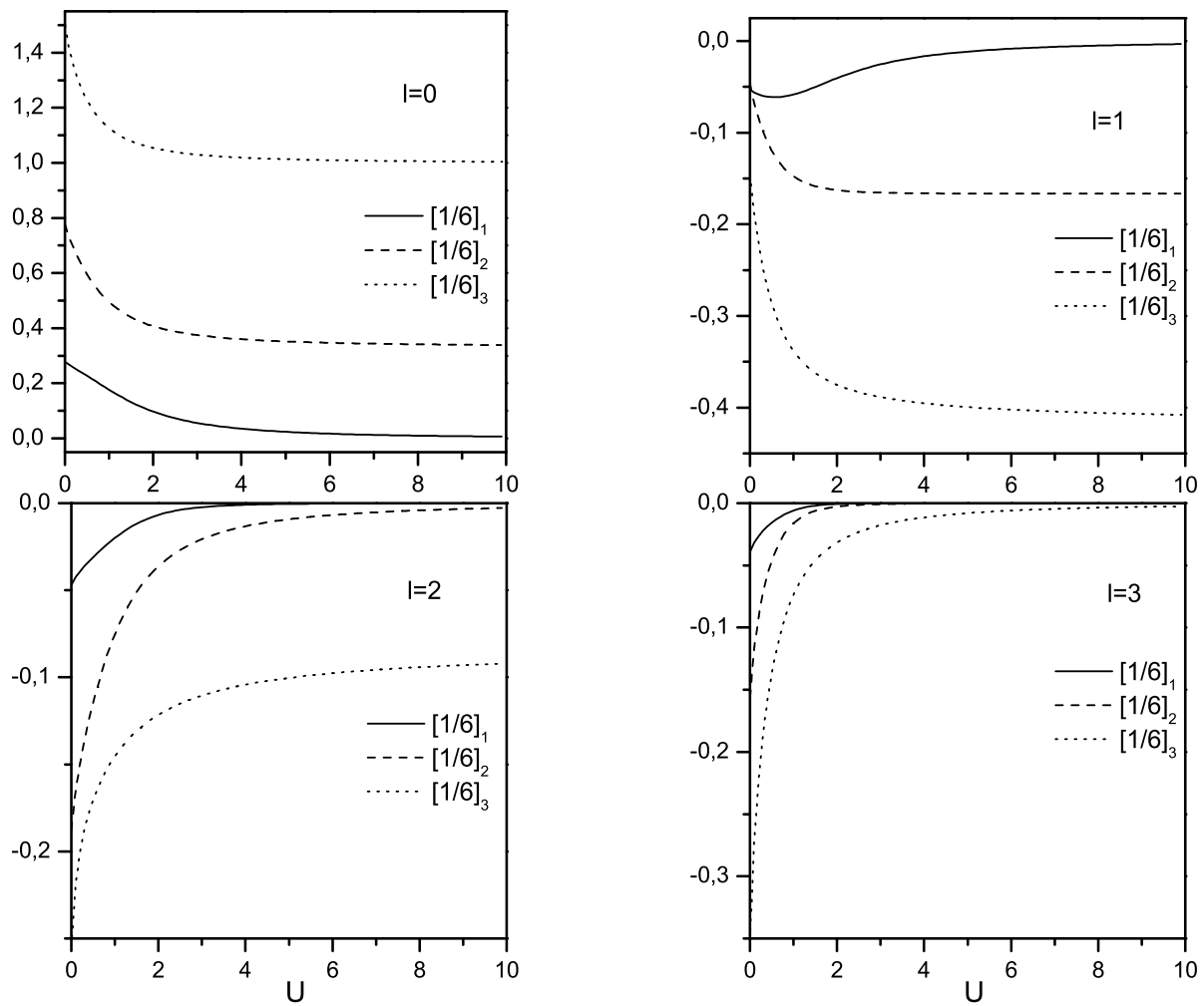


Figure 12: Infinite chain limit of $\mathcal{S}(l)$, given by (23), versus U , for different distances l , and different sets G .

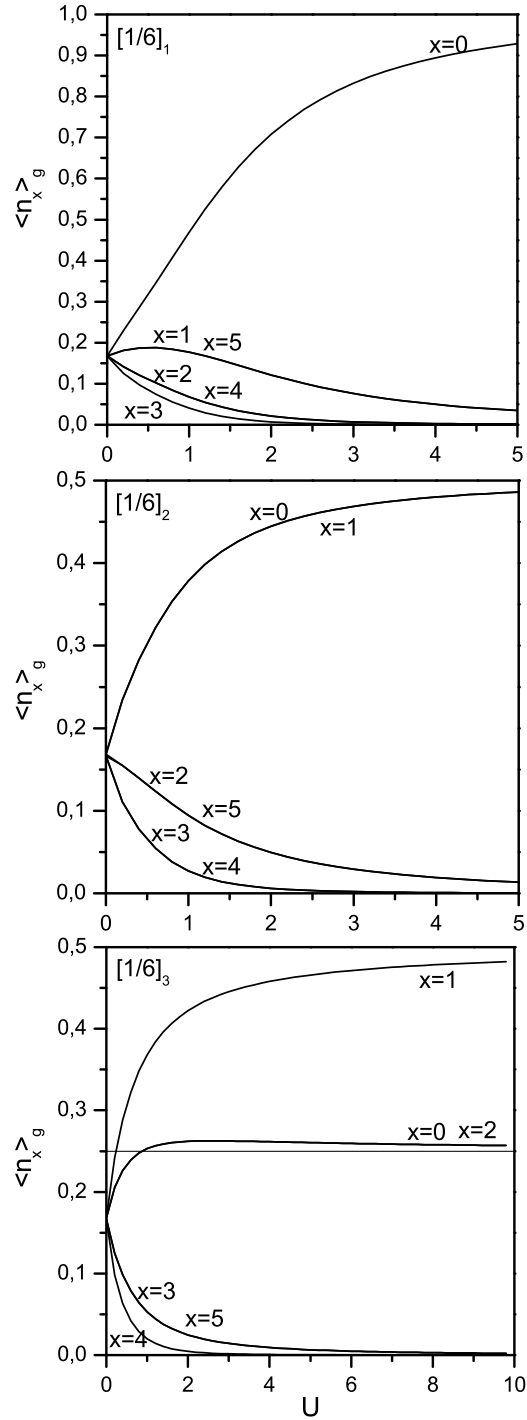


Figure 13: The local electron density in a fixed ion configuration g , versus position x , as a function of U . The ion configuration $g = 100000$ for $G = [1/6]_1$, $g = 110000$ for $G = [1/6]_2$, and $g = 111000$ for $G = [1/6]_3$.

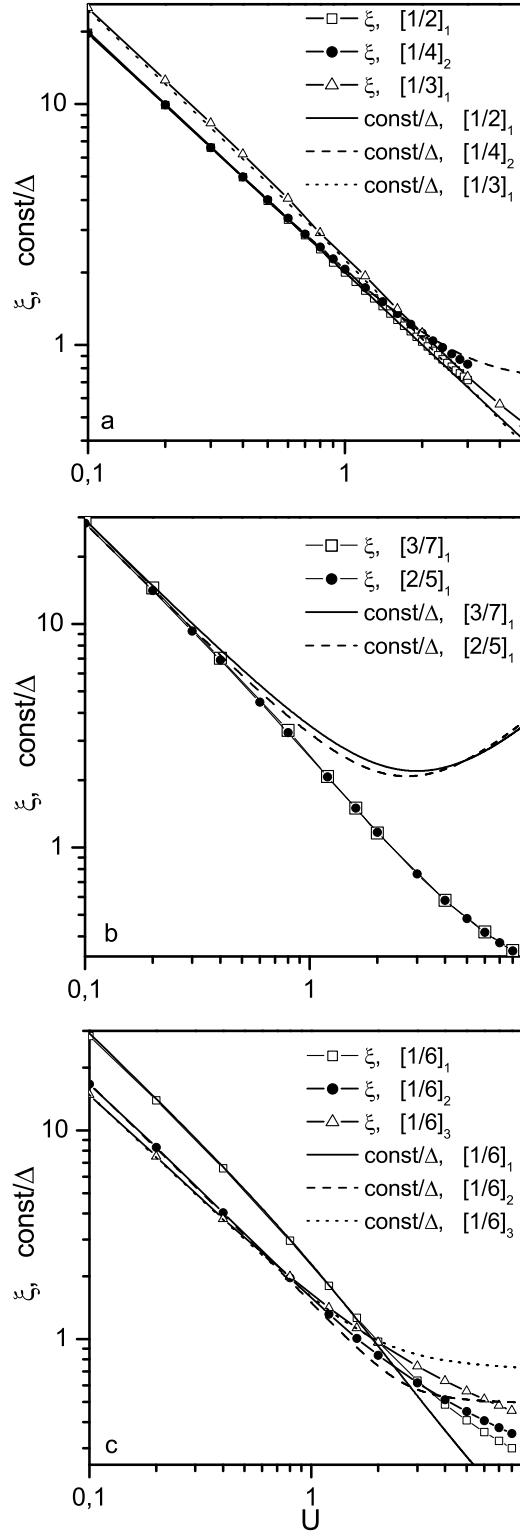


Figure 14: Numerically calculated correlation length ξ versus U , and numerically calculated $const\Delta^{-1}$, with $const$ adjusted so that $\xi \approx const\Delta^{-1}$, for different sets G . The ξ has been obtained from approximating the large-distance behaviour of $|\langle a_x^+ a_{x+l} \rangle|^2$ by $const \exp(-l/\xi)$.

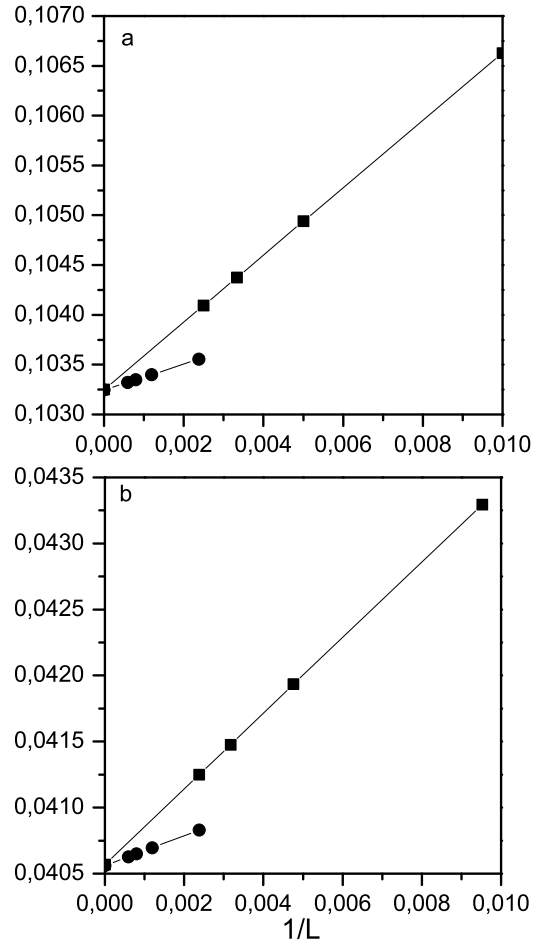


Figure 15: $\mathcal{P}_f(2\pi\rho_e)$, given by (31), and $\mathcal{P}'_f(2\pi\rho_e)$, given by (99), versus L^{-1} , for $U = 2$, and $G = [1/2]_1$ (a), $G = [3/7]_1$ (b). Filled squares: $\mathcal{P}_f(2\pi\rho_e)$, filled circles: $\mathcal{P}'_f(2\pi\rho_e)$.

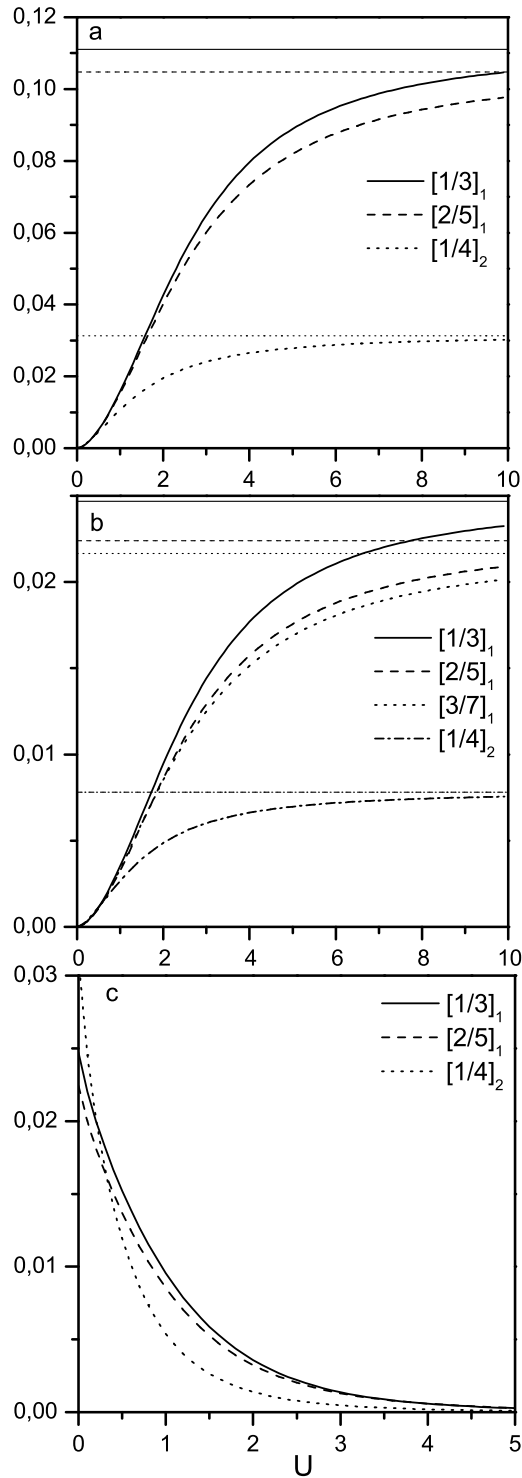


Figure 16: (a) $\mathcal{P}(2\pi\rho_\epsilon)$, given by (43), versus U , for different sets G , (b) \mathcal{L} , given by (44), versus U , for different sets G , (c) \mathcal{S} , given by (45), versus U , for different sets G . In (a) and (c) the plot corresponding to $G = [3/7]_1$ is missing, since it is indistinguishable from the plot for $G = [2/5]_1$.

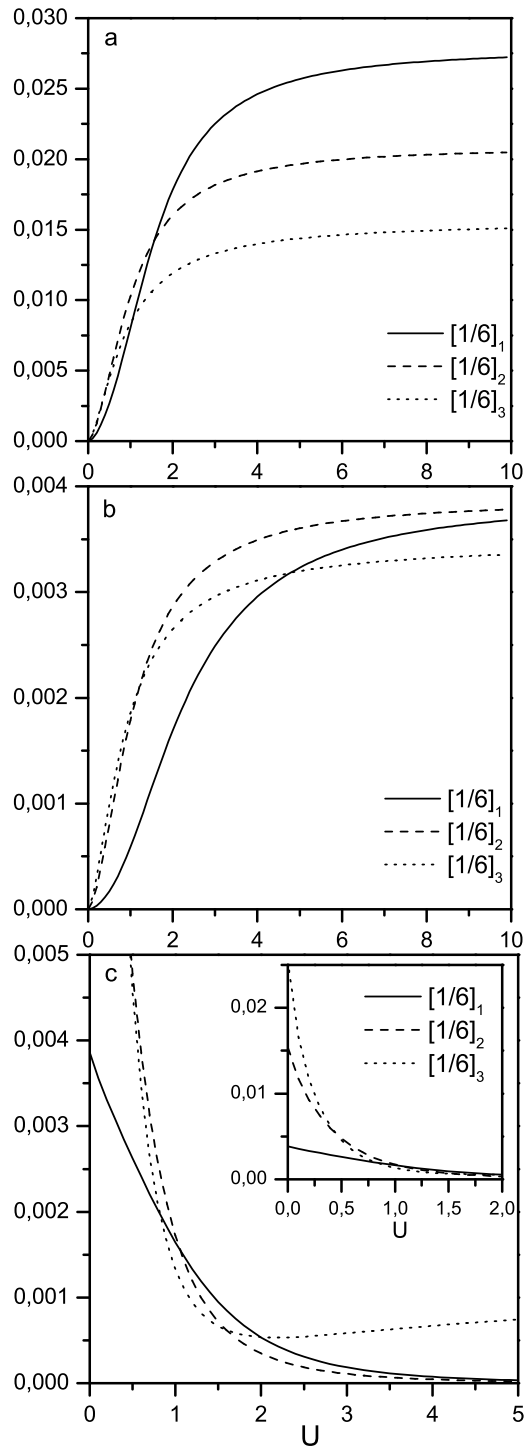


Figure 17: (a) $\mathcal{P}(2\pi\rho_e)$, given by (43), versus U , for different sets G , (b) \mathcal{L} , given by (44), versus U , for different sets G , (c) \mathcal{S} , given by (45), versus U , for different sets G .